이학박사학위논문

바이러스 핵산에 의한 제 1형 인터페론 신호전달 조절에 관한 연구

Study on the regulation of the type I interferon signaling mediated by viral nucleic acids

2017년 2월

서울대학교 대학원

생명과학부

서민지

CONTENTS

CONTENTS (*CONTINUED*)

LIST OF TABLES AND FIGURES

LIST OF ABBREVIATIONS

BTN3A1	Butyrophilin 3A1
MAP4	Microtubule-associated protein 4
TBK1	TANK-binding kinase 1
IRF3	IFN-regulatory factor 3
STING	Stimulator of interferon genes
MAVS	Mitochondrial antiviral signaling protein
IKK ε	Inhibitor of nuclear factor kappa-B kinase subunit epsilon
qRT-PCR	quantitative RT-PCR
poly I:C	Polyinosinic:polycytidylic acid
poly dA:Dt	Deoxyadenylic-thymidylic acid
HSV-1	Herpes simplex virus 1
RSV	Human respiratory syncytial virus
IFN-β	Interferon β
TNF-α	Tumor necrosis factor α
IP-10 (CXCL10)	Interferon gamma-induced protein 10
IFITM1	Interferon-induced transmembrane protein 1
MxA	Myxovirus resistance gene A
OasL	2'-5'-Oligoadenylate synthetase like

I. ABSTRACT

Minji Seo

School of
Biological science

The Graduate school

Seoul National University

The innate immune system detects viral nucleic acids and induces type I interferon (IFN) responses. The RNA- and DNA-sensing pathways converge on the TANK-binding kinase 1 (TBK1) and the transcription factor IFN-regulatory factor 3 (IRF3). Activation of the IFN signaling pathway is known to trigger the redistribution of key signaling molecules to punctate perinuclear structures, but the mediators of this spatiotemporal regulation have yet to be defined. Here, we identify BTN3A1 as a positive regulator of nucleic acid-mediated type I IFN signaling. Depletion of BTN3A1 inhibits the cytoplasmic nucleic acid- or virus-triggered activation of IFN-β production. In the resting state,

BTN3A1 is constitutively associated with TBK1. Stimulation with nucleic acids induces the redistribution of the BTN3A1-TBK1 complex to the perinuclear region, where BTN3A1 mediates the interaction between TBK1 and IRF3, leading to the phosphorylation of IRF3. Furthermore, we show that microtubule associated protein 4 (MAP4) controls the dynein-dependent transport of BTN3A1 in response to nucleic acid stimulation, thereby identifying MAP4 as an upstream regulator of BTN3A1. Thus, the depletion of either MAP4 or BTN3A1 impairs cytosolic DNA- or RNA-mediated type I IFN responses. Our findings demonstrate a critical role for MAP4 and BTN3A1 in the spatiotemporal regulation of TBK1, a central player in the intracellular nucleic acid sensing pathways involved in antiviral signaling.

Keywords: *BTN3A1, Nucleic acid, Type I IFN signaling, MAP4, Dynein, and TBK1-IRF3 axis*

Student Number: *2010-30934*

Ⅱ. INTRODUCTION

1. Type I IFN signaling

Type I IFN signaling is the most critical and powerful innate immune response to viral infection [1, 2]. The innate immune system comprises a limited number of germline encoded receptors, called pattern recognition receptors (PRR), to recognize viral pathogen-associated molecular patterns (PAMPs) as ‘nonself’. Toll-like receptors (TLRs) are the first identified class of PRR that recognize extracellular and endosomal PAMPs [3]. TLR 3, 7, 8, and 9 are TLRs able to recognize viral nucleic acid species. TLR3 is known to recognize dsRNA, while TLR7 and TLR8 are responsible for sensing ssRNA, and TLR9 recognizes unmethylated CpG DNA [4]. Cytosolic PRRs include the RIG-I-like receptors (RLRs), the nucleotide-binding domain and leucine-rich repeat containing molecules (NLRs) and intracellular sensors for DNA [5-7]. The RLR family consists of three receptors, retinoic acid inducible gene I (RIG-I), melanoma differentiation associated gene 5 (MDA5) and laboratory of genetics and physiology 2 (LGP2) [8]. RIG-I recognizes 5’-triphosphate RNA and short forms of dsRNA, whereas MDA5 mainly senses longer dsRNA species [9, 10]. Cytosolic sensors recognizing DNA include cyclic GMP-AMP synthase (cGAS), Mre11, IFI16, and DDX41 [11-14]. Type I IFN signaling pathways initiating from those DNA or RNA sensors are apparently converged on stimulator of interferon genes (STING), or mitochondrial antiviral signaling protein (MAVS) respectively. Even though PRRs recruit different adaptor proteins like STING or

MAVS, both STING and MAVS activate protein kinase TBK1 essential for type I IFN expression [15-17]. Active TBK1 phosphorylates IRF3, the transcription factor, leading to translocation of IRF3 from cytoplasm to nucleus and then activate the transcription of type I IFN genes [18].

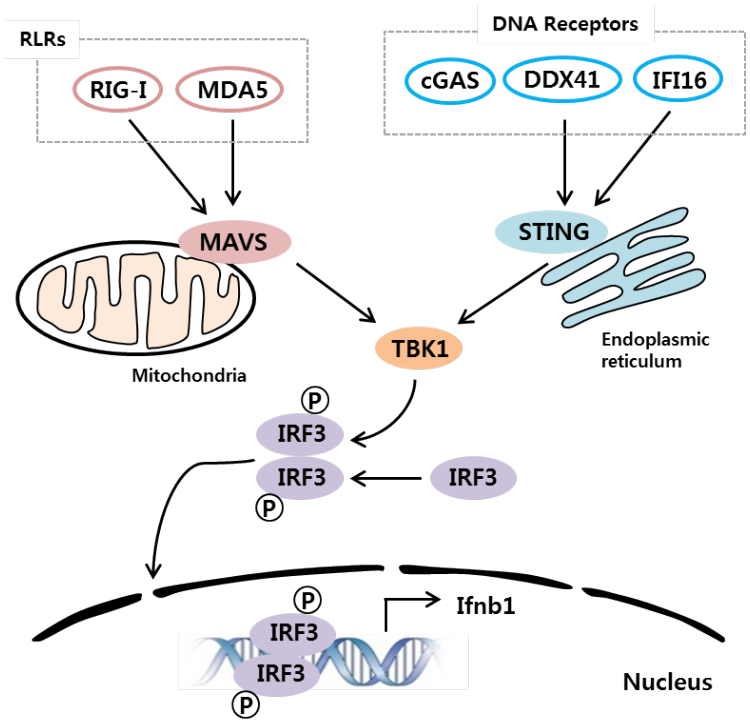
RLRs
RIG-I
MDA5
DNA Receptors
cGAS
DDX41
IFI16
MAVS
STING
Mitochondria
Endoplasmic reticulum
TBK1
P
IRF3
IRF3
IRF3
P
P
IRF3
IRF3
P
Ifnb1
Nucleus

Figure 1. Cytosolic nucleic acids mediated type I IFN response

Retinoic acid-inducible gene I (RIG-I) and melanoma differentiation associated protein 5 (MDA5) detect ssRNA and dsRNA, and then induce type I interferons (IFNs) through mitochondrial antiviral signaling protein (MAVS), TANK-binding kinase 1 (TBK1) and IFN-regulatory factor 3 (IRF3). DNA is sensed by cGAS, DDX41, and IFNgamma-inducible protein 16 (IFI16). All of these receptors signal through the endoplasmic reticulum (ER)-resident protein, stimulator of IFN genes protein (STING), which acts upstream of TBK1. Then, activated TBK1 phosphorylates IRF3 and it triggers their dimerization and nuclear translocation, where they form active transcriptional complexes that bind to IFN stimulation response elements (ISRE) and activate type I IFN genes expression.

2. Butyrophilin (BTN) family

The first butyrophilin was described in the 1980s, when BTN1A1 was identified and shown to have a role in lactation. Additional butyrophilin family members have been identified, many of which are conserved between human and mice. To date, the butyrophilin family is known to have 13 members including BTN1A1, BTN2A1, BTN2A2, BTN2A3, BTN3A1, BTN3A2, BTN3A3, butyrophilin-like protein 2 (BTNL2), BTNL3, BTNL8, BTNL9, BTNL10 and SKINT-like (STINKTL) [19]. The structural features of butyrophilins indicate that these proteins are very closely related to the B7 superfamily of co-stimulatory molecules. Similar to the B7 family, members of the butyrophilin family typically have two extracellular immunoglobulin domains, a transmembrane region and a B30.2 intracellular signaling domain [20]. Many butyrophilins are expressed by immune cells and by cells that closely interact with immune cells. Butyrophilins and butyrophilin-like molecules are emerging as novel regulators of immune responses in mice and humans.

Human gene	Mouse gene	Expression pattern	Interacting cells or receptor expression	Functions	Refs
BTN1A1	*Btn1a1*	Mammary glands, thymic stromal cells and B cells	Activated T cells and macrophages	Regulation of milk droplet secretion	[21, 22]
BTN2A1		Intestinal epithelial cells and broad immune cell expression, Colon, HUVEC	DCs, DC-SIGN		[23, 24]
BTN2A2	*Btn2a2*	Dendritic cells, monocytes, B cells and thymic epithelial cells	Activated T cells	Inhibition of T cell activation	[21, 24, 25]
BTN2A3	*Unknown*	Unknown	Unknown	Unknown	
BTN3A1		Stressed cells, malignant cells and broad immune cell expression	B cells and T cells	Immunosuppressive: inhibitor of T cell proliferation and cytokine secretion	[26-28]
BTN3A2		Malignant cells and broad	Unknown	Unknown	[24, 26,

		immune cell expression			29]
BTN3A3		Broad immune cell expression	Unknown	Unknown	[24, 26]
	Btnl1	Intestinal epithelial cells and macrophages	Activated T cells, B cells and dendritic cells	Modulator of intestinal epithelial cell–T cell interaction, Immunosuppressive: inhibitor of T cell activation	[30, 31]
BTNL2	*Btnl2*	Intestinal epithelial cells, plasmacytoid dendritic cells and macrophages	T cells, B cells and vascular endothelium	Immunosuppressive: negative regulator of T cell proliferation and cytokine production	[32, 33]
BTNL3		Neutrophils	Unknown	Unknown	[24]
	Btnl4	Intestinal epithelial cells	Unknown	Unknown	[30]
	Btnl5	Unknown	Unknown	Unknown	
	Btnl6	Intestinal epithelial cells	Unknown	Unknown	[30]
	Btnl7	Unknown	Unknown	Unknown	
BTNL8		Neutrophils	Resting T cells	Unknown	[34]
BTNL9	*Btnl9*	B cells	Activated T cells, B cells, dendritic cells	Unknown	[24, 31]

			and macrophages		
BTNL10	*Btnl10*	Unknown	Unknown	Unknown	
SKINTL		Unknown	Unknown	Unknown	
	Skint1	Thymic epithelial cells		Unknown	[35]
	Skint2	Broad expression in lymphoid and non-lymphoid tissues	Activated T cells and antigen-presenting cells	Unknown	[36]
	Skint3-11	Unknown	Unknown	Unknown	

Table 1. Expression patterns and function of BTN and Btnl family members

3. Microtubule associated proteins and motor proteins

Microtubules form a dynamic and polarized cytoskeleton. In most cell types, microtubule plus ends grow dynamically out from the microtubule-organizing center (MTOC), where the minus ends are more stably tethered. Microtubules mediate the transport of vesicles and organelles via the microtubule motor proteins kinesins and dyneins. Kinesins are a large superfamily with 45 members and are involved in trafficking events directed towards the cell periphery. By contrast, cytoplasmic dynein is used to shuttle proteins to the minus end of the microtubule, as in the case of trafficking from the ER to the Golgi [37]. Microtubule-associated proteins (MAPs) are proteins that interact with the microtubules of the cellular cytoskeleton. MAPs interact with the tubulin subunits that consist of microtubules to control their stability. A large variety of MAPs have been identified in many different cell types. MAPs have been found to carry out a wide range of functions including both stabilizing and destabilizing microtubules. Also, they guide microtubules towards specific cellular locations and mediate the interactions of microtubules with other proteins in the cell. There are a few reports that have been described a link between microtubules and cytosol nucleic acid mediated type I IFN signaling. The detection of nucleic acids in antiviral host defense seems to depend on microtubules bound to GEF-H1 [38]. Given the relation between trafficking and type I IFN signaling, it is likely that the microtubule-dependent transport of key components of the type I IFN signaling pathway is crucial for inducing antiviral immune responses. However, the dependence of microtubules on downstream components of nucleic acid sensing is currently unknown.

Ⅲ. RESULTS

1. Identification and characterization of BTN3A1 as a novel regulator of type I IFN response

We first attempted to identify regulatory genes required for the activation of type I IFN responses. Screening a siRNA library targeting interferon-inducible genes or genes with functional domains implicated in innate immune responses (Table 2) identified butyrophilin 3A1 (BTN3A1) as a positive regulator of type I IFN responses. The depletion of BTN3A1 significantly attenuated IFN-β secretion in virus-infected or dsDNA-stimulated cells without affecting cell viability (Figure 2). BTN3A1 specifically interacted with STING, TBK1, and IRF3 (Figure 3). Unlike the previously identified cytosolic DNA sensors IFI16 and DDX41 [13, 14], BTN3A1 did not exhibit DNA binding activity (Figure 4).

To characterize the physiological function of BTN3A1 in nucleic acid-induced responses, we employed a knockdown strategy involving four distinct siRNAs targeting the human BTN3A1 gene. Differentiated THP-1 cells treated with these siRNAs exhibited a considerable reduction in BTN3A1 expression. Moreover, the mRNA expression level of IFN-β, TNF-α, and OasL induced by dsDNA was significantly decreased in BTN3A1-silenced cells. All four siRNAs targeting BTN3A1 had remarkable silencing effects without affecting cell viability (Figure 5). Thus, a pool of four siRNAs was used for further study. The knockdown of BTN3A1 led to a substantial reduction in the production of IFN-β and TNF-α upon induction by cytosolic nucleic acids (Figure 6). The

knockdown of BTN3A1 did not inhibit the production of IFN-β and TNF-α when coupled with stimulation by TLR ligands, LPS and poly I:C (Figure 7). These results indicate that BTN3A1 is specifically involved in the cytosolic nucleic acid-mediated type I IFN response. To determine whether the BTN3A1-mediated induction of type I IFNs occurs under more physiological conditions, a similar analysis was conducted in primary cells derived from human peripheral blood mononuclear cells (PBMC). We infected monocyte-derived macrophages (MDMs) with the DNA virus HSV-1 or the RNA virus Sendai. Reduced expression levels of IFN-β and TNF-α were observed in BTN3A1 knockdown MDMs, supporting the hypothesis that BTN3A1 acts as a positive regulator of type I IFN responses induced by cytosolic DNA and RNA (Figure 8). The human butyrophilin family consists of BTN1A1, BTN2A1, BTN2A2, BTN2A3, BTN3A1, BTN3A2, and BTN3A3. Among these family members, only siBTN3A1 effectively reduced IFN-β mRNA and protein, revealing the specificity of BTN3A1 in type I IFN responses (Figure 9).

Characteristic	Gene Number
NACHT Domain	24
LRR Domain	200
PADD_DAPIN Domain	22
CARD Domain	33
SPRY Domain	80
BIR Domain	8
Interferon Inducible Genes	60
Location : Peroxisome	50
Total	**477**

Table 2. siRNA library used in this study

The siRNA library was designed to target interferon-inducible genes and genes with functional domains implicated in regulating innate immune responses such as NACHT domain, leucine-rich repeat domain, DAPIN domain, CARD domains, B30.2/SPRY domain, BIR domain and genes localized to the peroxisome. The siRNA library includes 477 genes. Each gene is targeted by four independent siRNAs to reduce off-target effects.

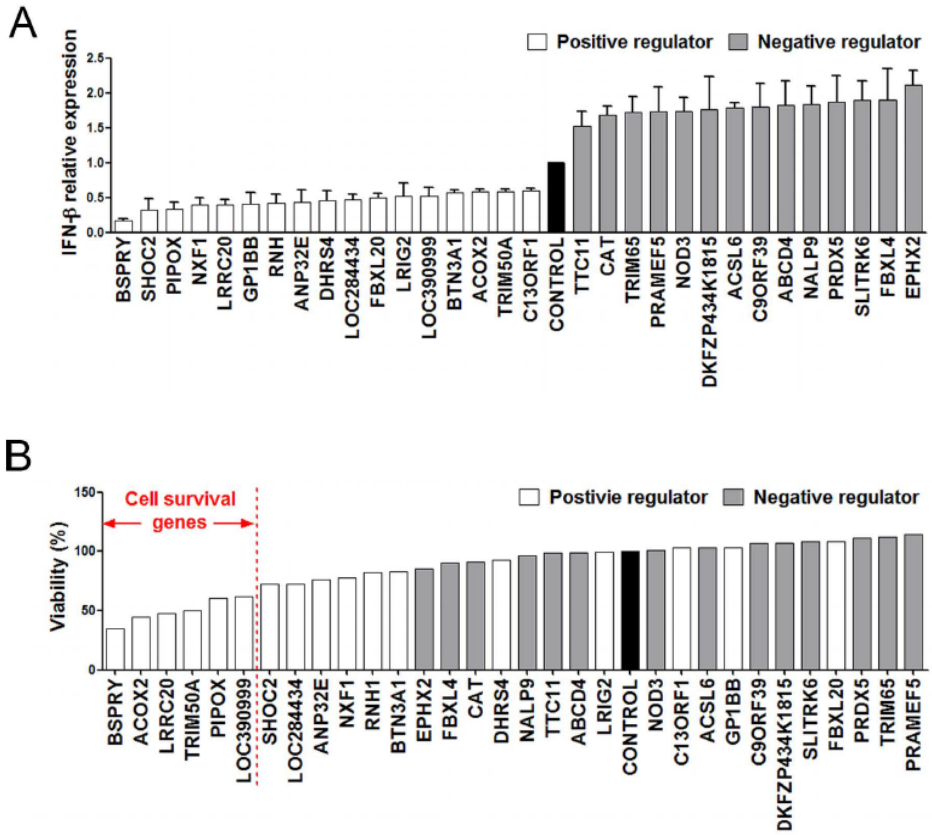
A
Positive regulator
Negative regulator
IFN-β relative expression
2.5
2.0
1.5
1.0
0.5
0.0
BSPRY
SHOC2
PIPOX
NXF1
LRRC20
GP1BB
RNH
ANP32E
DHRS4
LOC284434
FBXL20
LRIG2
LOC390999
BTN3A1
ACOX2
TRIM50A
C13ORF1
CONTROL
TTC11
CAT
TRIM65
PRAMEF5
NOD3
DKFZP434K1815
ACSL6
C9ORF39
ABCD4
NALP9
PRDX5
SLITRK6
FBXL4
EPHX2
B
Cell survival genes
Postivie regulator
Negative regulator
Viability (%)
150
100
50
0
BSPRY
ACOX2
LRRC20
TRIM50A
PIPOX
LOC390999
SHOC2
LOC284434
ANP32E
NXF1
RNH1
BTN3A1
EPHX2
FBXL4
CAT
DHRS4
NALP9
TTC11
ABCD4
LRIG2
CONTROL
NOD3
C13ORF1
ACSL6
GP1BB
C9ORF39
DKFZP434K1815
SLITRK6
FBXL20
PRDX5
TRIM65
PRAMEF5

Figure 2. The putative positive and negative regulators identified through siRNA screening

(A) The putative positive and negative regulators identified through primary siRNA screening detected by ELISA analysis of IFN-β production in THP-1 cells treated with siRNA enlisted in Table 2 for 72 hr, and then stimulated with poly dA:dT for 6 hr. (B) The viability of positive and negative regulators was assessed using the indicated siRNA-transfected THP-1 cells by measuring the level of cellular ATP.

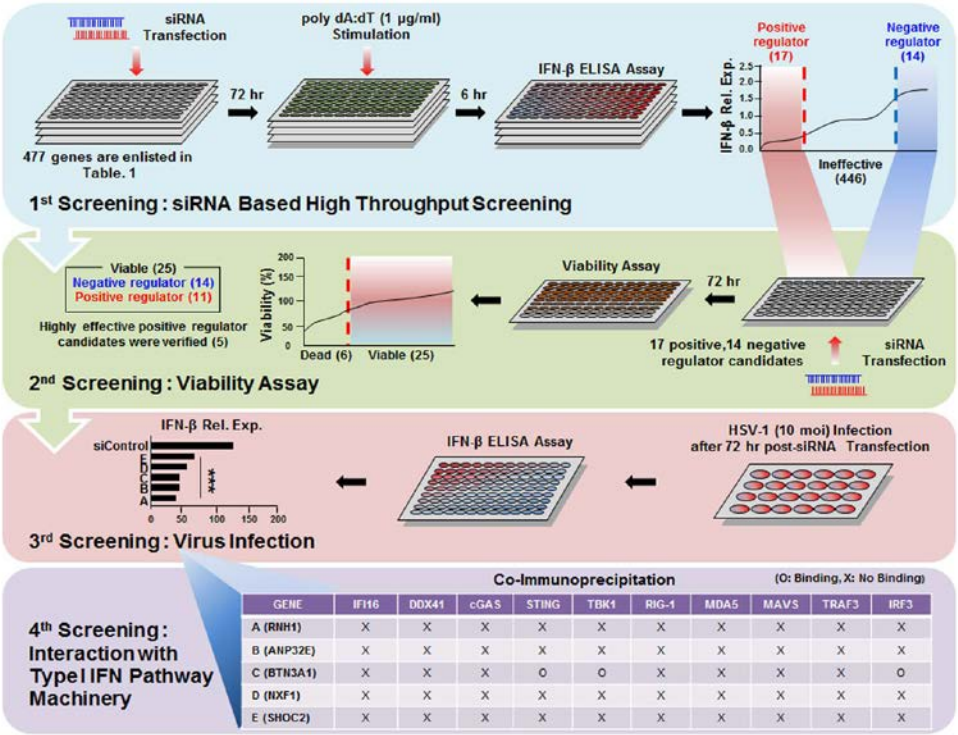

GENE	IFI16	DDX41	cGAS	STING	TBK1	RIG-I	MDA5	MAVS	TRAF3	IRF3
A (RNH1)	X	X	X	X	X	X	X	X	X	X
B (ANP32E)	X	X	X	X	X	X	X	X	X	X
C (BTN3A1)	X	X	X	O	O	X	X	X	X	O
D (NXF1)	X	X	X	X	X	X	X	X	X	X
E (SHOC2)	X	X	X	X	X	X	X	X	X	X

Figure 3. A schematic representation of the four screening steps

1: ELISA analysis of IFN-β in THP-1 cells transfected with siRNA (Table 2) and then stimulated with dsDNA. 2: Viability analysis of THP-1 cells silenced with siRNA targeting putative candidate genes by measuring cellular ATP level. 3: ELISA and real time PCR analysis of IFN-β in THP-1 cells treated with siRNA targeting selected positive regulator candidate genes, followed by infection with 10 MOI HSV-1. 4: Immunoprecipitation and immunoblot analysis of HEK293T cells co-transfected with the indicated combinations of expression plasmids.

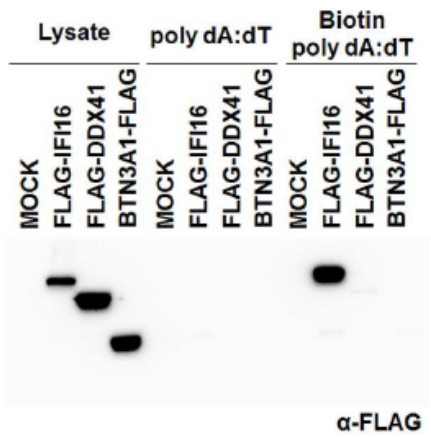
Lysate
poly dA:dT
Biotin
poly dA:dT
MOCK
FLAG-IFI16
FLAG-DDX41
BTN3A1-FLAG
MOCK
FLAG-IFI16
FLAG-DDX41
BTN3A1-FLAG
MOCK
FLAG-IFI16
FLAG-DDX41
BTN3A1-FLAG
α-FLAG

Figure 4. BTN3A1 does not exhibit DNA binding activity

SDS-PAGE of extracts of HEK293T cells expressing mock, FLAG-IFI16, FLAG-DDX41, or BTN3A1-FLAG and treated with poly dA:dT or biotinylated poly dA:dT for 2 hr, followed by immunoprecipitation using streptavidin beads.

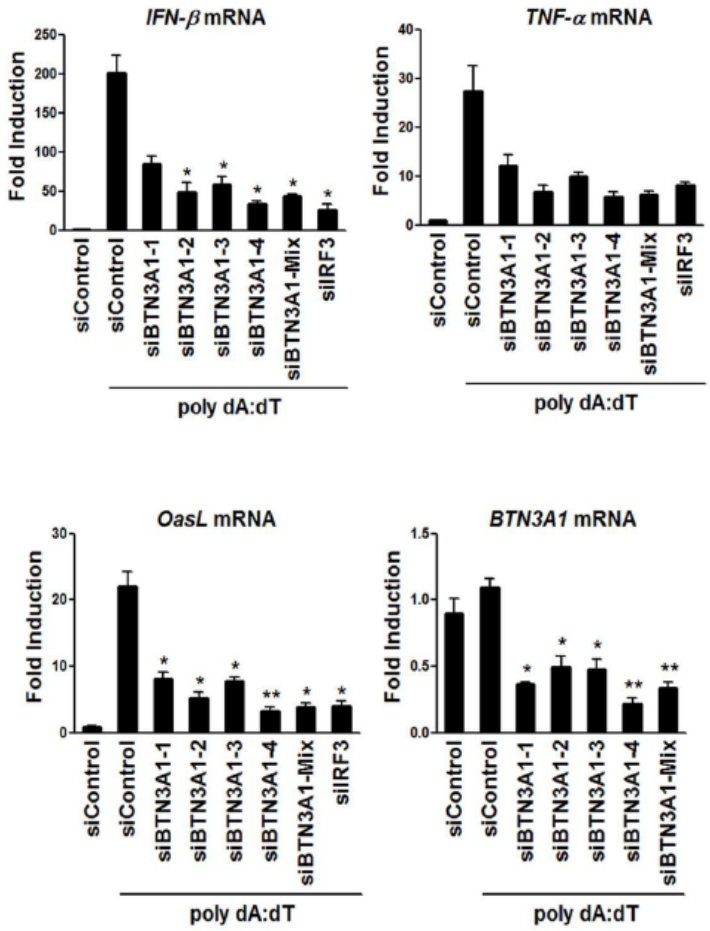
IFN-β mRNA
Fold Induction
250
200
150
100
50
0
siControl
siControl
siBTN3A1-1
siBTN3A1-2
siBTN3A1-3
siBTN3A1-4
siBTN3A1-Mix
siIRF3
poly dA:dT
TNF-α mRNA
Fold Induction
40
30
20
10
0
siControl
siControl
siBTN3A1-1
siBTN3A1-2
siBTN3A1-3
siBTN3A1-4
siBTN3A1-Mix
siIRF3
poly dA:dT
OasL mRNA
Fold Induction
30
20
10
0
siControl
siControl
siBTN3A1-1
siBTN3A1-2
siBTN3A1-3
siBTN3A1-4
siBTN3A1-Mix
siIRF3
poly dA:dT
BTN3A1 mRNA
Fold Induction
1.5
1.0
0.5
0.0
siControl
siControl
siBTN3A1-1
siBTN3A1-2
siBTN3A1-3
siBTN3A1-4
siBTN3A1-Mix
poly dA:dT

Figure 5. BTN3A1 is required for type I IFN signaling

qRT-PCR analysis of IFN-β, TNF-α, OasL and BTN3A1 mRNA in THP-1 cells treated with control siRNA, siRNAs targeting BTN3A1, or siRNA targeting IRF3, followed by stimulation with poly dA:dT for 4 hr. siIRF3 serves as an internal positive control. Viability analysis of the indicated siRNA-transfected THP-1 cells via measuring intracellular ATP level. * $P<0.05$ and ** $P<0.01$ versus cells transfected with control siRNA (Student's t-test). Data are representative of three independent experiments.

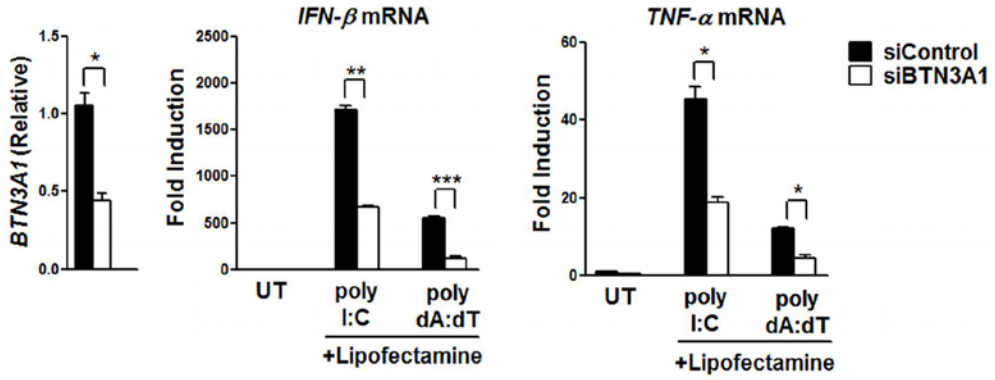
BTN3A1 (Relative)
1.5
1.0
0.5
0.0
*
IFN-β mRNA
Fold Induction
2500
2000
1500
1000
500
0
**
***
UT
poly I:C
poly dA:dT
+Lipofectamine
TNF-α mRNA
Fold Induction
60
40
20
0
*
*
UT
poly I:C
poly dA:dT
+Lipofectamine
siControl
siBTN3A1

Figure 6. BTN3A1 is necessary for cytosolic nucleic acid-mediated type I IFN response

qRT-PCR analysis of BTN3A1, IFN-β, and TNF-α mRNA in THP-1 cells transfected with non-targeting siRNA (siControl) or BTN3A1-targeting siRNA (siBTN3A1) that were subsequently left untreated (UT) or treated with intracellular poly I:C or poly dA:dT for 4 hr. * $P<0.05$, ** $P<0.01$ and *** $P<0.001$ versus cells transfected with siControl (Student's t-test). The data are representative of three independent experiments.

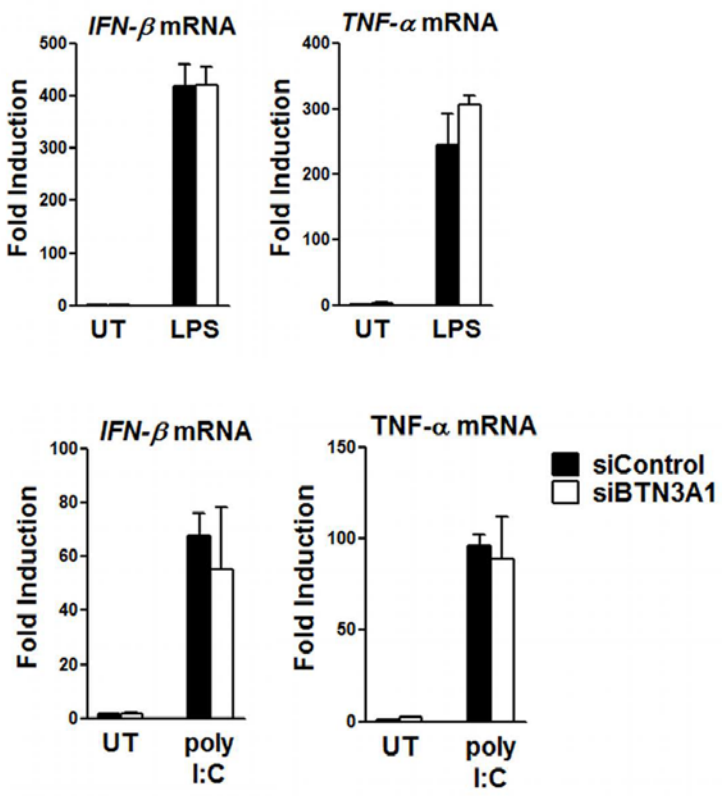
IFN-β mRNA
Fold Induction
500
400
300
200
100
0
UT
LPS
TNF-α mRNA
Fold Induction
400
300
200
100
0
UT
LPS
IFN-β mRNA
Fold Induction
100
80
60
40
20
0
UT
poly I:C
TNF-α mRNA
Fold Induction
150
100
50
0
UT
poly I:C
siControl
siBTN3A1

Figure 7. BTN3A1 is dispensable for TLR mediated type I IFN response

qRT-PCR analysis of IFN-β and TNF-α mRNA in THP-1 cells treated with siControl or siBTN3A1, followed by incubation with LPS or extracellular poly I:C for 2 hr.

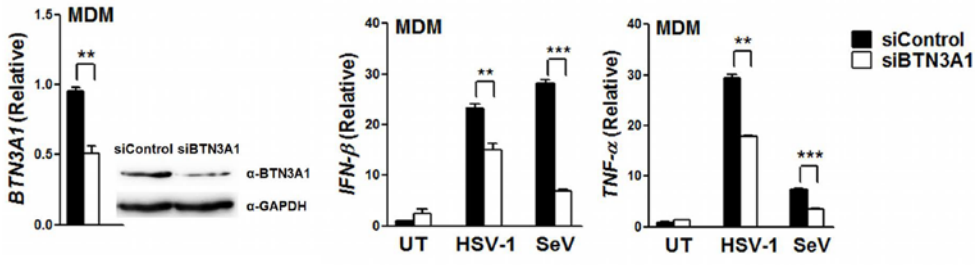
MDM
BTN3A1 (Relative)
1.5
1.0
0.5
0.0
**
siControl siBTN3A1
α-BTN3A1
α-GAPDH
MDM
IFN-β (Relative)
40
30
20
10
0
**
***
UT
HSV-1
SeV
MDM
TNF-α (Relative)
40
30
20
10
0
**
***
UT
HSV-1
SeV
siControl
siBTN3A1

Figure 8. BTN3A1 acts as a positive regulator of type I IFN responses induced by either DNA or RNA virus infection

qRT-PCR analysis of IFN-β and TNF-α mRNA in MDMs silenced by siControl or siBTN3A1 using electroporation, followed by infection with HSV-1 (10 MOI) or SeV (1 MOI) for 4 hr. Immunoblot and qRT-PCR analyses of the knockdown of endogenous BTN3A1 in MDMs treated with siControl or siBTN3A1 were also performed. ** $P<0.01$ and *** $P<0.001$ versus cells transfected with siControl (Student's t-test). The data are representative of three independent experiments.

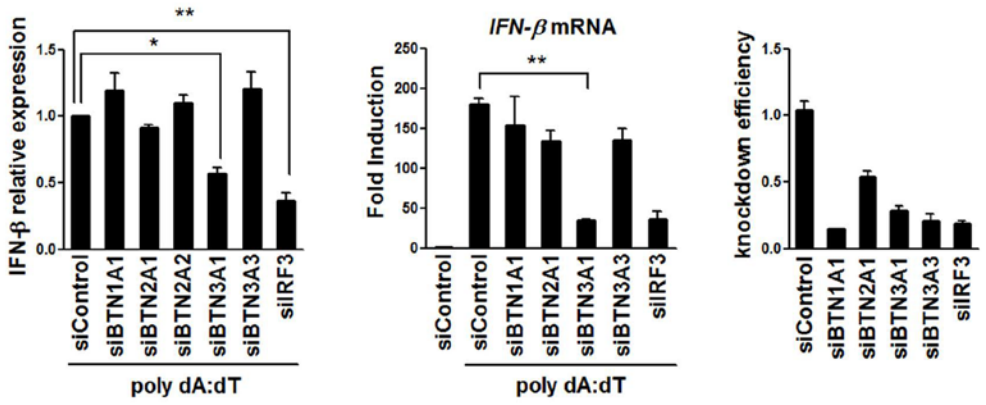
IFN-β relative expression
1.5
1.0
0.5
0.0
**
*
siControl
siBTN1A1
siBTN2A1
siBTN2A2
siBTN3A1
siBTN3A3
siIRF3
poly dA:dT
IFN-β mRNA
Fold Induction
250
200
150
100
50
0
**
siControl
siControl
siBTN1A1
siBTN2A1
siBTN3A1
siBTN3A3
siIRF3
poly dA:dT
knockdown efficiency
1.5
1.0
0.5
0.0
siControl
siBTN1A1
siBTN2A1
siBTN3A1
siBTN3A3
siIRF3

Figure 9. The specific regulation of BTN3A1 in type I IFN responses

ELISA for IFN-β protein and qRT-PCR analysis of IFN-β, BTN isoforms and IRF3 mRNA in THP-1 cells treated with the indicated siRNA and then stimulated with dsDNA for 6 hr. * P<0.05, ** P<0.01 and *** P<0.001 versus cells transfected with siControl (Student's t-test). The data are representative of three independent experiments. * P<0.05 and ** P<0.01 versus cells transfected with siControl (Student's t-test). The data are representative of three independent experiments.

2. BTN3A1 regulates the phosphorylation of IRF3

To investigate the functional mechanism of BTN3A1 in nucleic acid-mediated type I IFN signaling, we generated stable THP-1 cell lines in which BTN3A1 was knocked down using lentiviral shRNA constructs. The reduced expression of BTN3A1 was confirmed at the protein and mRNA levels (Figure 10). THP-1 cells treated with shBTN3A1 exhibited impaired production of IFN-β compared to THP-1 cells treated with shControl following treatment with poly I:C, poly dA:dT, STING ligands, c-di-AMP and c-di-GMP or infection with HSV-1 or Sendai virus (Figure 10). MDA5 preferentially detects the long form of poly I:C (>1000 bp), whereas RIG-I preferentially senses its short form (>300 and <1000 bp) [9, 10]. BTN3A1 was essential for triggering type I IFN responses to both the long and short forms of poly I:C (Figure 11), suggesting that BTN3A1 acts downstream of RNA detection. Similarly, the knockdown of BTN3A1 suppressed cytoplasmic poly dA:dT-, c-di-AMP- or c-di-GMP-induced activation of IFN-β, suggesting that the regulatory function of BTN3A1 is downstream of STING. BTN3A1 was crucial for the production of IFN-β during challenges with the DNA virus HSV-1 or the RNA viruses SeV and RSV, regardless of the MOI (multiplicity of infection) (Figure 11). The effect of BTN3A1 was extended to the induction of TNF-α, an indicator of NF-κB activation, and interferon stimulatory genes (ISGs) (Figure 12 and Figure 13). Collectively, these observations suggest that BTN3A1 controls type I IFN signaling downstream of RNA sensors and STING.

During the nucleic acid-mediated immune response, the production of IFN-β depends on the TBK1-induced phosphorylation of IRF3, followed by IRF3 dimerization and finally nuclear translocation of IRF3. The phosphorylation of

S386 and S396 is critical for IRF3 dimerization and its nuclear translocation, respectively [39]. The decreased phosphorylation of IRF3 at both sites was observed in shBTN3A1-transduced THP-1 cells with poly dA:dT (Figure 14A). Similar results were obtained when shBTN3A1-transduced cells were incubated with various doses of poly I:C or poly dA:dT for different durations (Figure 15). Cell fractionation analysis revealed that BTN3A1 knockdown significantly inhibited the nuclear accumulation of phosphorylated IRF3 (Figure 14B). Notably, BTN3A1 knockdown did not affect TBK1 phosphorylation, suggesting that BTN3A1 might be a downstream effector of phosphoTBK1 (Figure 16). The reduced activation of IFN-β due to BTN3A1 knockdown was rescued by exogenous BTN3A1 expression (Figure 17). To verify the data obtained from RNAi-mediated knockdown approach, we generated BTN3A1 knockout HeLa cell lines by using CRISPR/Cas9 genome editing system (Figure 18). Knockout of BTN3A1 resulted in decreased IFN-β and IP-10 induction in nucleic acid-stimulated and virus-infected cells (Figure 19). In addition, we detected less IFN-β expression in BTN3A1 knockout cells during the time course of infection (Figure 20). Phosphorylation of IRF3 was impaired in the BTN3A1 knockout cells (Figure 21A). Knockout of BTN3A1 inhibited the cytoplasmic to nuclear translocation of IRF3 that is induced by nucleic acid treatment or virus infection (Figure 21B). We obtained essentially the same results as observed with RNAi-mediated knockdown system, with more pronounced phenotypes in knockout approach.

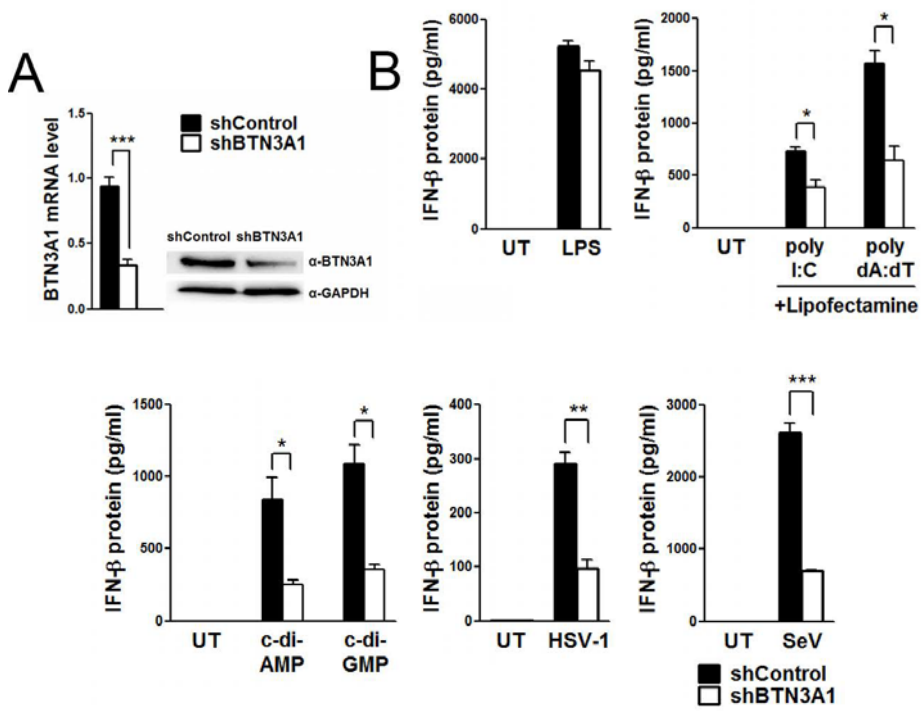
A
BTN3A1 mRNA level
1.5
1.0
0.5
0.0
***
shControl
shBTN3A1
shControl shBTN3A1
α-BTN3A1
α-GAPDH
B
IFN-β protein (pg/ml)
6000
4000
2000
0
UT
LPS
2000
1500
1000
500
0
*
*
UT
poly I:C
poly dA:dT
+Lipofectamine
1500
1000
500
0
*
*
UT
c-di-AMP
c-di-GMP
400
300
200
100
0
**
UT
HSV-1
3000
2000
1000
0
***
UT
SeV
shControl
shBTN3A1

Figure 10. BTN3A1 is required for RLR-mediated type I IFN response

(A) qRT-PCR and immunoblot analyses of THP-1 cells treated with shRNA with a scrambled sequence (shControl) or with shRNA targeting BTN3A1 (shBTN3A1) without stimulation. (B) ELISA for IFN-β in THP-1 cells transfected with shControl or shBTN3A1 and then left untreated (UT) or stimulated with LPS, poly I:C, poly dA:dT, c-di-AMP or c-di-GMP or infected with HSV-1 or SeV for 6 hr. * $P<0.05$, ** $P<0.01$ and *** $P<0.001$ versus cells transfected with shControl (Student's t-test). The data are representative of three independent experiments.

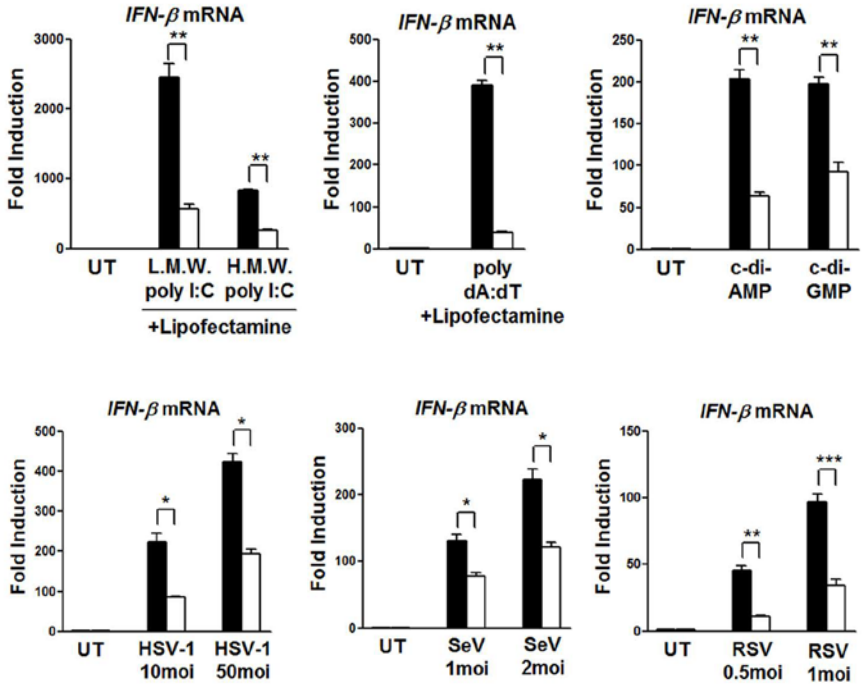
IFN-β mRNA
Fold Induction
3000
2000
1000
0
**
**
UT
L.M.W. poly I:C
H.M.W. poly I:C
+Lipofectamine
IFN-β mRNA
Fold Induction
500
400
300
200
100
0
**
UT
poly dA:dT
+Lipofectamine
IFN-β mRNA
Fold Induction
250
200
150
100
50
0
**
**
UT
c-di-AMP
c-di-GMP
IFN-β mRNA
Fold Induction
500
400
300
200
100
0
*
*
UT
HSV-1 10moi
HSV-1 50moi
IFN-β mRNA
Fold Induction
300
200
100
0
*
*
UT
SeV 1moi
SeV 2moi
IFN-β mRNA
Fold Induction
150
100
50
0
**
***
UT
RSV 0.5moi
RSV 1moi

Figure 11. BTN3A1 controls type I IFN signaling downstream of RNA sensors and STING

qRT-PCR analysis of IFN-β mRNA in THP-1 cells treated with either shControl or shBTN3A1, followed by transfection with low molecular weight (L.M.W.) poly I:C, high molecular weight (H.M.W.) poly I:C, poly dA:dT, c-di-AMP or c-di-GMP or by infection with HSV-1, SeV or RSV for 6 hr. * $P<0.05$, ** $P<0.01$ and *** $P<0.001$ versus cells transfected with shControl (Student's t-test). The data are representative of three independent experiments.

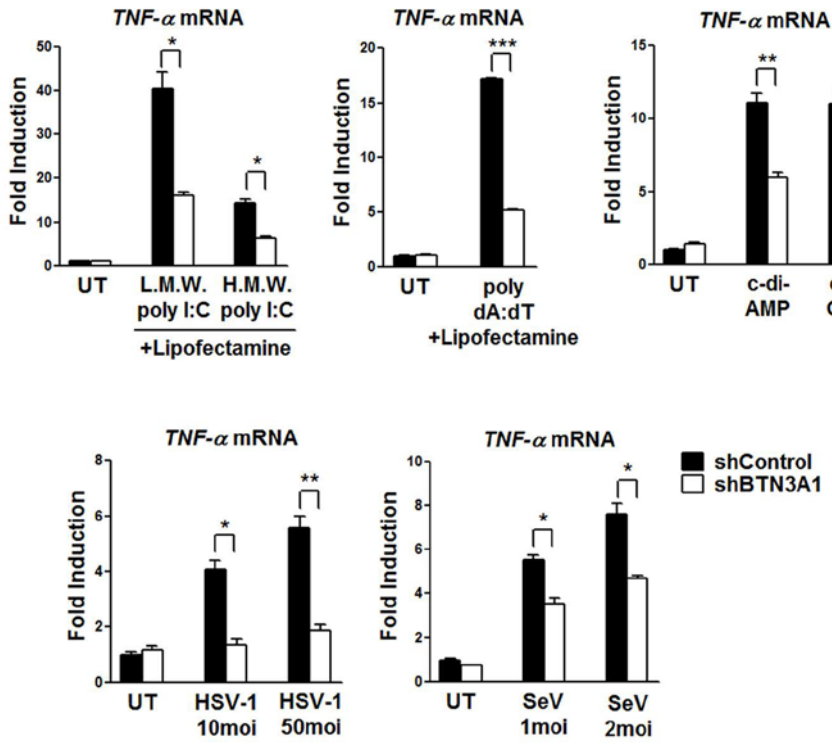
TNF-α mRNA
Fold Induction
50
40
30
20
10
0
*
*
UT
L.M.W. poly I:C
H.M.W. poly I:C
+Lipofectamine
TNF-α mRNA
Fold Induction
20
15
10
5
0
***
UT
poly dA:dT
+Lipofectamine
TNF-α mRNA
Fold Induction
15
10
5
0
**
**
UT
c-di-AMP
c-di-GMP
TNF-α mRNA
Fold Induction
8
6
4
2
0
*
**
UT
HSV-1 10moi
HSV-1 50moi
TNF-α mRNA
Fold Induction
10
8
6
4
2
0
*
*
UT
SeV 1moi
SeV 2moi
shControl
shBTN3A1

Figure 12. BTN3A1 is required for the induction of *TNF-α* in response to nucleic acid stimulation

qRT-PCR analysis of TNF-α mRNA in THP-1 cells treated with either shControl or shBTN3A1, followed by transfection with low molecular weight (L.M.W.) poly I:C, high molecular weight (H.M.W.) poly I:C, poly dA:dT, c-di-AMP or c-di-GMP or by infection with HSV-1, or SeV for 6 hr. * $P<0.05$, ** $P<0.01$ and *** $P<0.001$ versus cells transfected with shControl (Student's t-test). The data are representative of three independent experiments.

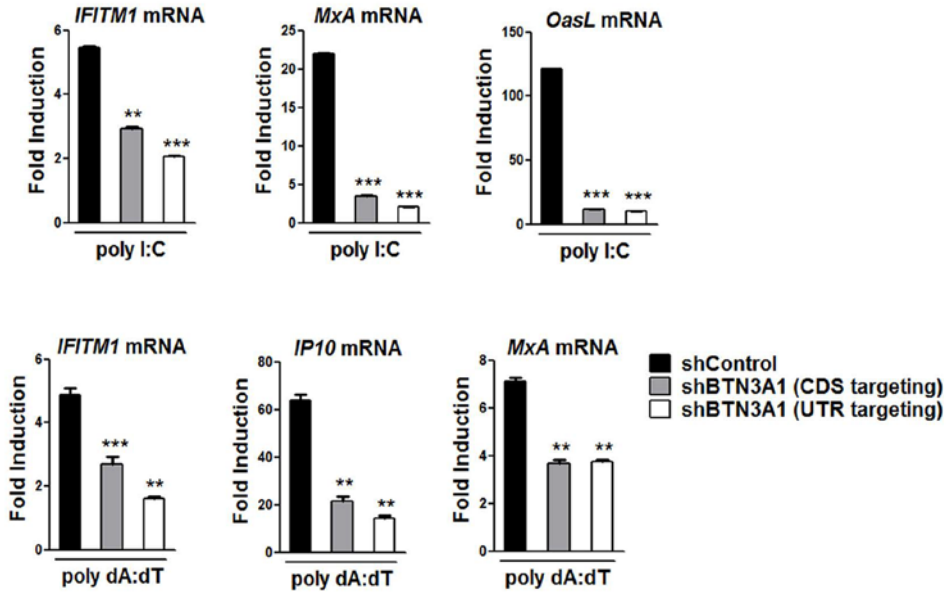
IFITM1 mRNA
MxA mRNA
OasL mRNA
Fold Induction
poly I:C
IFITM1 mRNA
IP10 mRNA
MxA mRNA
poly dA:dT
shControl
shBTN3A1 (CDS targeting)
shBTN3A1 (UTR targeting)

Figure 13. BTN3A1 is necessary for induction of IFN-stimulatory genes

qRT-PCR analysis of IFITM1, MxA, OasL, and IP10 mRNA in THP-1 cells treated with control shRNA or shRNA targeting the coding sequence (CDS) or 3' UTR of BTN3A1, followed by stimulation with poly I:C or poly dA:dT for 4 hr. ** $P<0.01$ and *** $P<0.001$ versus cells transfected with shControl (Student's t-test). The data are representative of three independent experiments.

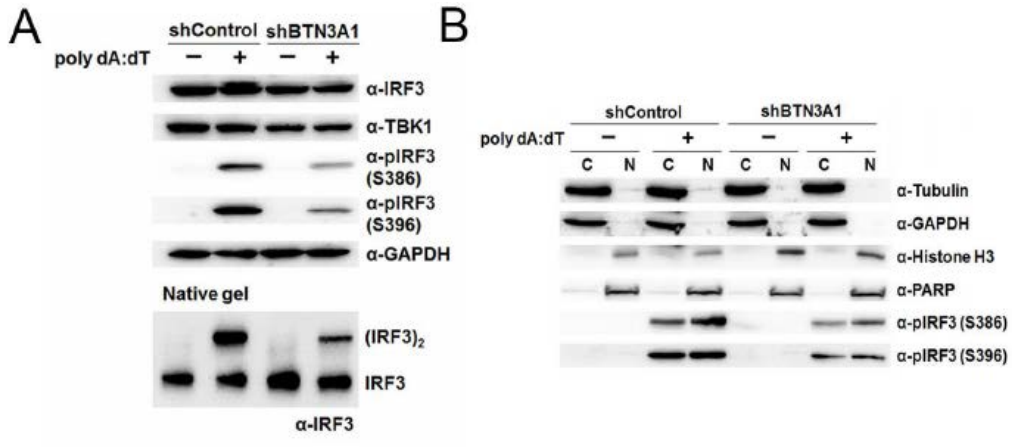
A
shControl
shBTN3A1
poly dA:dT
−
+
−
+
α-IRF3
α-TBK1
α-pIRF3 (S386)
α-pIRF3 (S396)
α-GAPDH
Native gel
(IRF3)2
IRF3
α-IRF3
B
shControl
shBTN3A1
poly dA:dT
C
N
α-Tubulin
α-GAPDH
α-Histone H3
α-PARP
α-pIRF3 (S386)
α-pIRF3 (S396)

Figure 14. BTN3A1 regulates the phosphorylation and nuclear translocation of IRF3

(A) SDS PAGE and native PAGE in THP-1 cells transfected with shControl or shBTN3A1, followed by stimulation for 3 hr with poly dA:dT. (B) Immunoblot assay for α-Tubulin, GAPDH, histone H3, PARP, and phospholRF3 in the cytosol (C) or the nucleus (N) of THP-1 cells treated with shControl or shBTN3A1 and then stimulated with poly dA:dT for 3 hr.

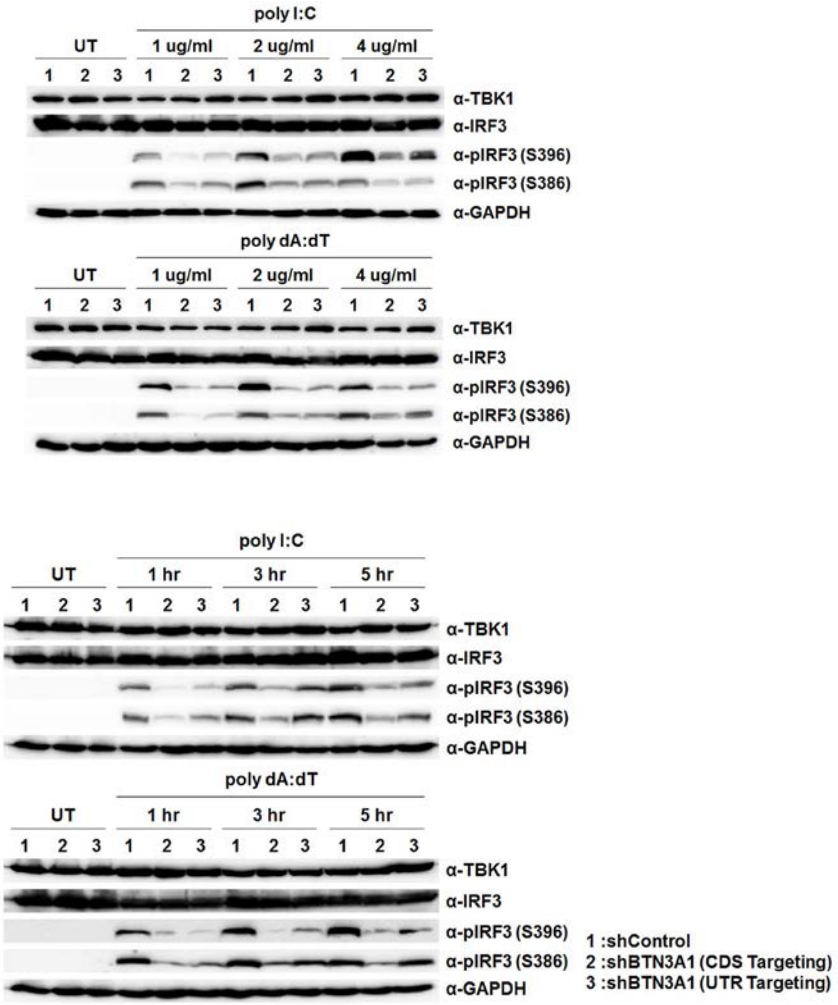
poly I:C
UT
1 ug/ml
2 ug/ml
4 ug/ml
1 2 3 1 2 3 1 2 3 1 2 3
α-TBK1
α-IRF3
α-pIRF3 (S396)
α-pIRF3 (S386)
α-GAPDH
poly dA:dT
UT
1 ug/ml
2 ug/ml
4 ug/ml
1 2 3 1 2 3 1 2 3 1 2 3
α-TBK1
α-IRF3
α-pIRF3 (S396)
α-pIRF3 (S386)
α-GAPDH
poly I:C
UT
1 hr
3 hr
5 hr
1 2 3 1 2 3 1 2 3 1 2 3
α-TBK1
α-IRF3
α-pIRF3 (S396)
α-pIRF3 (S386)
α-GAPDH
poly dA:dT
UT
1 hr
3 hr
5 hr
1 2 3 1 2 3 1 2 3 1 2 3
α-TBK1
α-IRF3
α-pIRF3 (S396)
α-pIRF3 (S386)
α-GAPDH
1 :shControl
2 :shBTN3A1 (CDS Targeting)
3 :shBTN3A1 (UTR Targeting)

Figure 15. BTN3A1 controls the phosphorylation of IRF3

Immunoblot analysis of total and phosphorylated IRF3 in THP-1 cells treated with control shRNA or shRNA targeting the coding sequence (CDS) or 3' UTR of BTN3A1, followed by stimulation with poly I:C or poly dA:dT at the indicated doses and time periods.

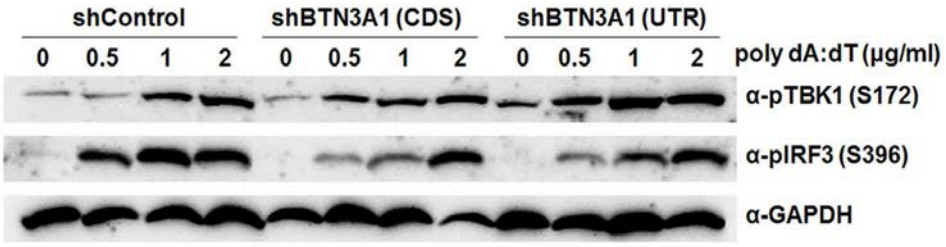
shControl
shBTN3A1 (CDS)
shBTN3A1 (UTR)
0 0.5 1 2 0 0.5 1 2 0 0.5 1 2
poly dA:dT (μg/ml)
α-pTBK1 (S172)
α-pIRF3 (S396)
α-GAPDH

Figure 16. BTN3A1 knockdown does not affect TBK1 phosphorylation

Immunoblot analysis of phosphorylated TBK1 and IRF3 in THP-1 cells treated with shControl or shRNAs targeting the coding sequence (CDS) or 3' UTR of BTN3A1, followed by stimulation for 3 hr with poly dA:dT at the indicated doses.

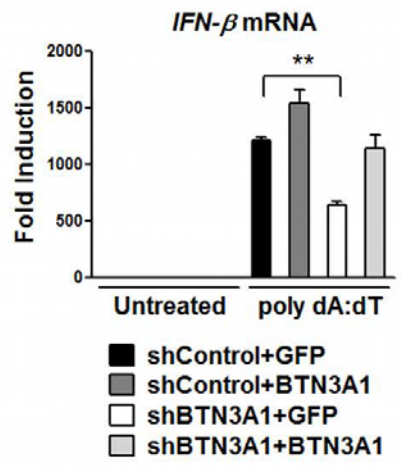
IFN-β mRNA
Fold Induction
2000
1500
1000
500
0
**
Untreated
poly dA:dT
shControl+GFP
shControl+BTN3A1
shBTN3A1+GFP
shBTN3A1+BTN3A1

Figure 17. Restoration of BTN3A1 expression leads to the *IFN-β* production

qRT- PCR analysis of IFN-β in THP-1 cells treated with shControl or shBTN3A1 and then stimulated for 4 hr with poly dA:dT after reconstitution with GFP or BTN3A1. ** P<0.01 versus cells transfected with shControl (Student's t-test). The data are representative of three independent experiments.

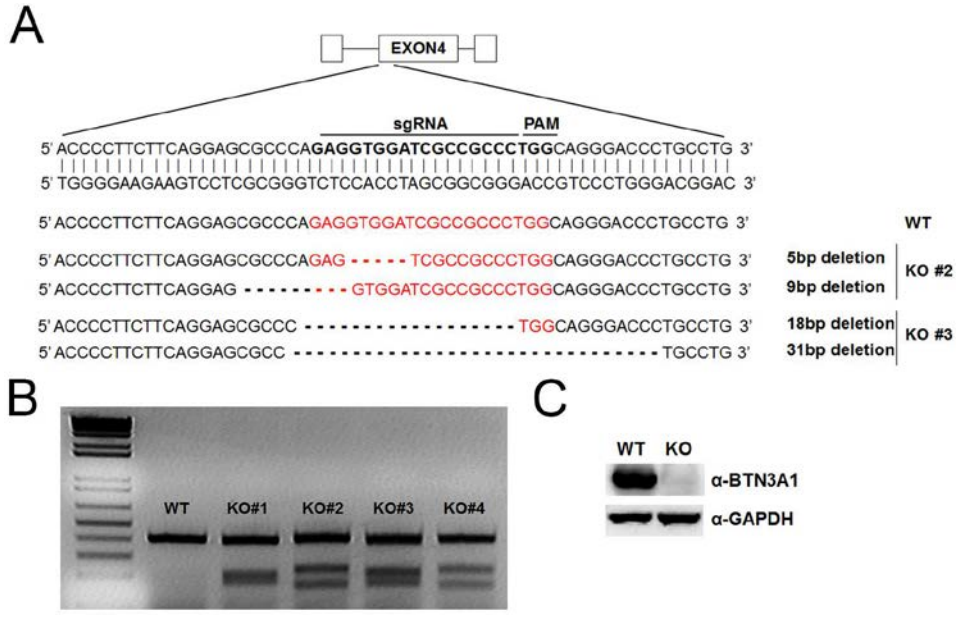
A
EXON4
sgRNA
PAM
5' ACCCCTTCTTCAGGAGCGCCCAGAGGTGGATCGCCGCCCTGGCAGGGACCCTGCCTG 3'
5' TGGGGAAGAAGTCCTCGCGGGTCTCCACCTAGCGGCGGGACCGTCCCTGGGACGGAC 3'
5' ACCCCTTCTTCAGGAGCGCCCAGAGGTGGATCGCCGCCCTGGCAGGGACCCTGCCTG 3'
WT
5' ACCCCTTCTTCAGGAGCGCCCAGAG - - - - - TCGCCGCCCTGGCAGGGACCCTGCCTG 3'
5bp deletion
5' ACCCCTTCTTCAGGAG - - - - - - - - - GTGGATCGCCGCCCTGGCAGGGACCCTGCCTG 3'
9bp deletion
KO #2
5' ACCCCTTCTTCAGGAGCGCCC - - - - - - - - - - - - - - - - - TGGCAGGGACCCTGCCTG 3'
18bp deletion
5' ACCCCTTCTTCAGGAGCGCC - TGCCTG 3'
31bp deletion
KO #3
B
WT
KO#1
KO#2
KO#3
KO#4
C
WT
KO
α-BTN3A1
α-GAPDH

Figure 18. BTN3A1 knockout using a CRISPR/Cas9 approach

(A) Schematic depiction of the BTN3A1 locus. The sequence targeted by sgRNA is indicated by bold letters. Sequences of the targeted BTN3A1 alleles of the two obtained BTN3A1 knockout cell lines. (B) T7E1 cleavage assay for mutation detection in individual clones. (C) Immunoblot assay of the extracts from WT and BTN3A1 KO HeLa cells.

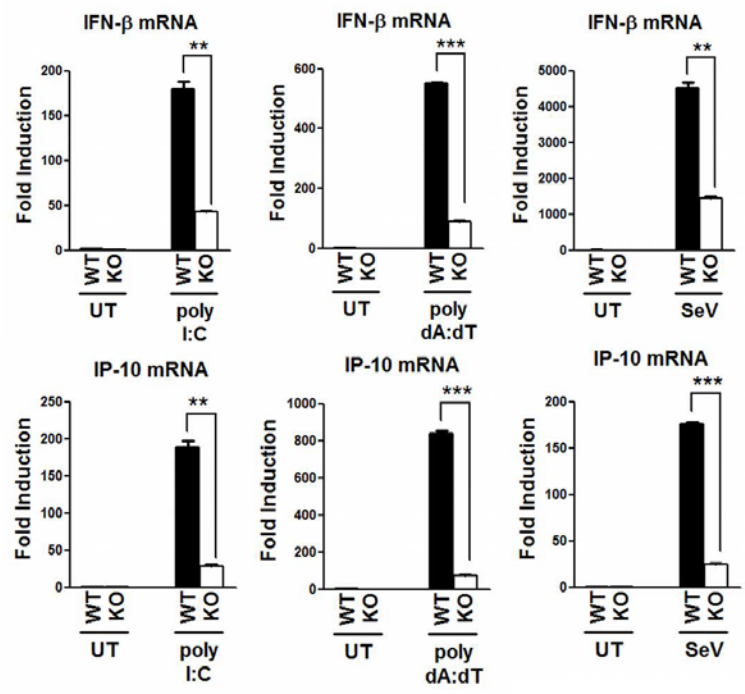
IFN-β mRNA
Fold Induction
200
150
100
50
0
**
WT
KO
UT
poly
I:C
IFN-β mRNA
Fold Induction
600
400
200
0
***
WT
KO
UT
poly
dA:dT
IFN-β mRNA
Fold Induction
5000
4000
3000
2000
1000
0
**
WT
KO
UT
SeV
IP-10 mRNA
Fold Induction
250
200
150
100
50
0
**
WT
KO
UT
poly
I:C
IP-10 mRNA
Fold Induction
1000
800
600
400
200
0
***
WT
KO
UT
poly
dA:dT
IP-10 mRNA
Fold Induction
200
150
100
50
0
***
WT
KO
UT
SeV

Figure 19. BTN3A1 is necessary for induction of *IFN-β* and *IL-10*

qRT-PCR analysis of IFN-β and IP-10 mRNA in wild-type (WT) and BTN3A1 knockout (KO) HeLa cells transfected with poly I:C, poly dA:dTor infected with SeV for 4 hr. ** P<0.01 and *** P<0.001 versus WT cells (Student ' s t-test). The data are representative of three independent experiments.

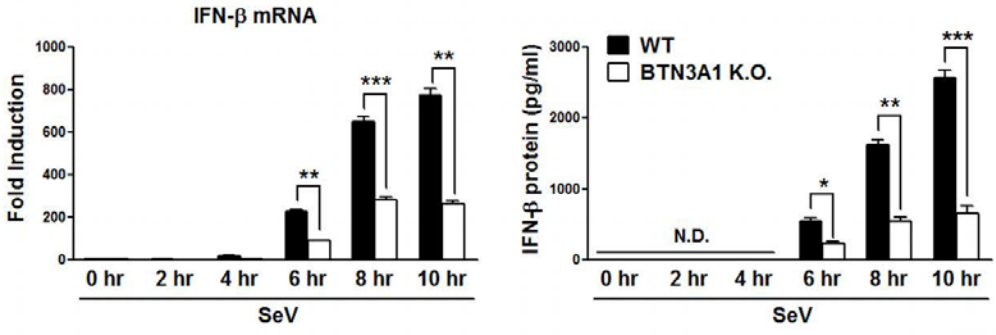
IFN-β mRNA
Fold Induction
1000
800
600
400
200
0
**
***
**
0 hr
2 hr
4 hr
6 hr
8 hr
10 hr
SeV
WT
BTN3A1 K.O.
IFN-β protein (pg/ml)
3000
2000
1000
0
N.D.
*
**
***
0 hr
2 hr
4 hr
6 hr
8 hr
10 hr
SeV

Figure 20. BTN3A1 is required for optimal expression of *IFN-β* in infection with SeV

qRT-PCR analysis of IFN-β in both WT and BTN3A1 KO cells inoculated with SeV at the indicated time periods. * P<0.05, ** P<0.01 and *** P<0.001 versus WT cells (Student's t-test). The data are representative of three independent experiments.

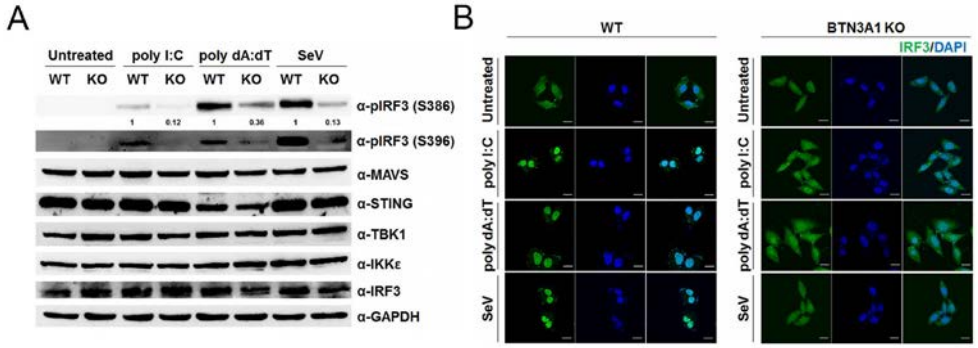
A
Untreated
poly I:C
poly dA:dT
SeV
WT KO WT KO WT KO WT KO
1 0.12 1 0.36 1 0.13
α-pIRF3 (S386)
α-pIRF3 (S396)
α-MAVS
α-STING
α-TBK1
α-IKKε
α-IRF3
α-GAPDH
B
WT
BTN3A1 KO
IRF3/DAPI
Untreated
poly I:C
poly dA:dT
SeV

Figure 21. BTN3A1 controls the phosphorylation and nuclear translocation of IRF3

(A) WT and BTN3A1 KO HeLa cells were stimulated for 3 hr with poly I:C, poly dA:dT or SeV. Cell lysates were analyzed by immunoblotting. (B) Confocal immunofluorescence microscopy of IRF3 (green) after stimulation with poly I:C, poly dA:dT or infection with SeV for 3 hr in WT and BTN3A1 KO HeLa cells. The nuclei of the cells were stained with DAPI (blue). Original magnification, 40x. The scale bar represents 20 μm.

3. BTN3A1 directs the interaction of TBK1 with IRF3

To determine whether endogenous BTN3A1 associates with components of the type I IFN signaling pathway, polyclonal antibodies against the B30.2 domain of BTN3A1 were raised in rabbits. THP-1 cells were left unstimulated or stimulated with poly I:C or poly dA:dT. Cell lysates were immunoprecipitated with anti-BTN3A1 antibody and then were subjected to immunoblotting analysis. We found that BTN3A1 interacts with TBK1 in both the resting and activated states. The association of BTN3A1 with IRF3 was undetectable in resting THP-1 cells, but their interaction was detected following nucleic acid stimulation. Neither MAVS nor IKKε was co-precipitated with BTN3A1 in a detectable manner. A weak interaction between BTN3A1 and STING was observed (Figure 22). We mapped the interacting domains of BTN3A1 and TBK1 using co-immunoprecipitation experiments with a series of deletion mutants lacking each functional domain. We found that SPRY/B30.2 domain of BTN3A1 is important for the interaction with TBK1 (Figure 23A). On the other hand, the binding interface of BTN3A1 was mapped to the CCD2 domain of TBK1 (Figure 23B). Because BTN3A1 interacts with both TBK1 and IRF3 in nucleic acid-stimulated cells, we explored the possibility that BTN3A1 influences TBK1-IRF3 association. We observed a strong association between TBK1 and IRF3 in shBTN3A1 cells after poly dA:dT stimulation. Knockdown of BTN3A1 markedly decreased the endogenous association between TBK1 and IRF3 in response to dsDNA stimulation, suggesting that BTN3A1 may act as an adaptor molecule in the formation of the TBK1-IRF3 complex, facilitating both the phosphorylation of IRF3 and signal transduction (Figure 24). Phosphorylation of MAVS and STING recruits IRF3 for its phosphorylation and activation by TBK1 [40]. To determine

if TBK1-IRF3-BTN3A1 complexes still form in MAVS or STING deficient cells, we expressed IRF3-2A mutant in which Ser385 and Ser386 are substituted with alanine, in MAVS knockdown or STING knockout cells. Since IRF3-2A mutant is unable to form a homodimer, it associates with its interacting partners more strongly [40]. Stimulation of these cells with poly I:C or poly dA:dT led to the association of IRF3-2A-FLAG with endogenous BTN3A1 and TBK1 (Figure 25, A and B, respectively). These results suggest that both MAVS and STING are dispensable for the formation of BTN3A1-TBK1-IRF3 complexes.

BTN3A1 localizes in the plasma membrane to present non-peptide prenyl pyrophosphate antigens to $\gamma\delta$ T cells [41, 42]. We analyzed the subcellular distribution of BTN3A1 by confocal microscopy in HeLa cells that were unstimulated or stimulated with poly I:C or poly dA:dT. In unstimulated HeLa cells, BTN3A1 exhibited a vesicle-like intracellular structure and colocalized with the tubulin diffused throughout the cytoplasm. Interestingly, BTN3A1 redistributed from a diffused expression pattern to a predominantly perinuclear localization after simulation with poly I:C or poly dA:dT (Figure 26). Ectopically expressed BTN3A1-GFP also displayed a similar subcellular distribution to endogenous BTN3A1. (Figure 27A). Nuclear and cytoplasmic fractionation revealed that BTN3A1 is predominantly localized to the cytoplasm regardless of nucleic acid stimulation (Figure 27B). To gain insight into the cellular function and dynamics of BTN3A1, we employed live cell imaging in HeLa cells expressing BTN3A1-GFP. Live-cell imaging revealed that BTN3A1 moves toward the perinuclear region under poly dA:dT stimulation, whereas the distribution of GFP remains largely unaffected (Figure 28).

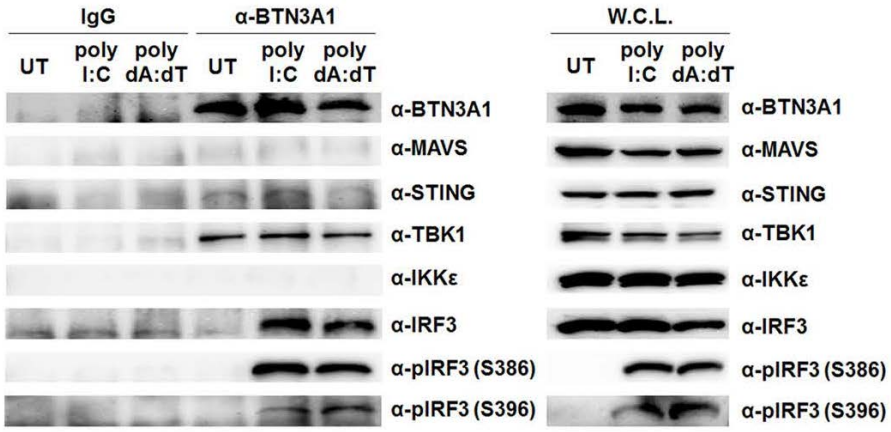
IgG
α-BTN3A1
W.C.L.
UT
poly I:C
poly dA:dT
UT
poly I:C
poly dA:dT
UT
poly I:C
poly dA:dT
α-BTN3A1
α-MAVS
α-STING
α-TBK1
α-IKKε
α-IRF3
α-pIRF3 (S386)
α-pIRF3 (S396)
α-BTN3A1
α-MAVS
α-STING
α-TBK1
α-IKKε
α-IRF3
α-pIRF3 (S386)
α-pIRF3 (S396)

Figure 22. BTN3A1 interacts with TBK1 and IRF3

Immunoassay of extracts from THP-1 cells untreated (UT) or treated with poly I:C or poly dA:dT for 3 hr, followed by immunoprecipitation with anti-IgG or anti-BTN3A1 antibodies and immunoblot analysis (antibodies, right margin). WCL, immunoblot analysis of whole cell lysates without immunoprecipitation.

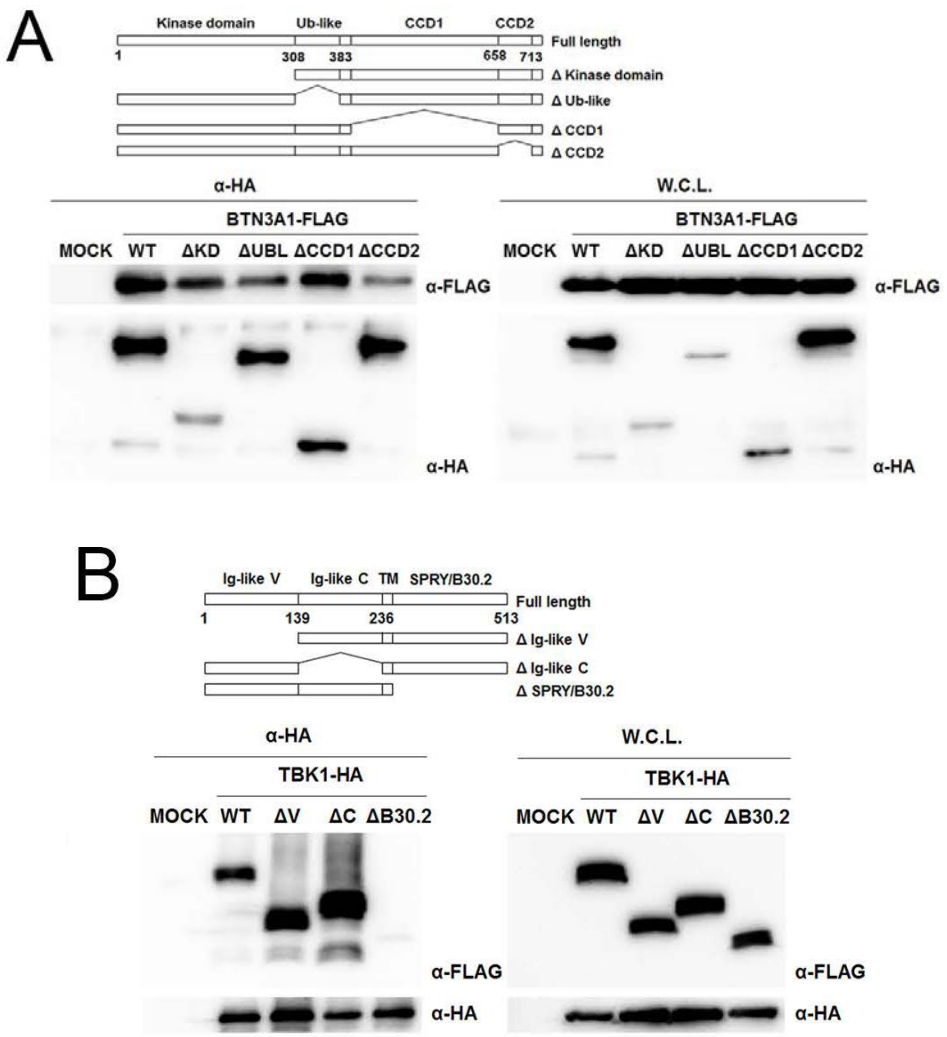
A
Kinase domain
Ub-like
CCD1
CCD2
Full length
1
308
383
658
713
Δ Kinase domain
Δ Ub-like
Δ CCD1
Δ CCD2
α-HA
W.C.L.
BTN3A1-FLAG
MOCK WT ΔKD ΔUBL ΔCCD1 ΔCCD2
α-FLAG
α-HA
B
Ig-like V
Ig-like C
TM
SPRY/B30.2
Full length
1
139
236
513
Δ Ig-like V
Δ Ig-like C
Δ SPRY/B30.2
α-HA
W.C.L.
TBK1-HA
MOCK WT ΔV ΔC ΔB30.2
α-FLAG
α-HA

Figure 23. CCD2 domain of TBK1 and B30.2 domain of BTN3A1 are important for their interaction

(A and B) Schematic representations of TBK1 and its deletion mutants (A) and BTN3A1 and its deletion mutants (B). The extracts from HEK293T cells co-transfected with the indicated combinations of expression plasmids were immunoprecipitated followed by immunoblot analysis.

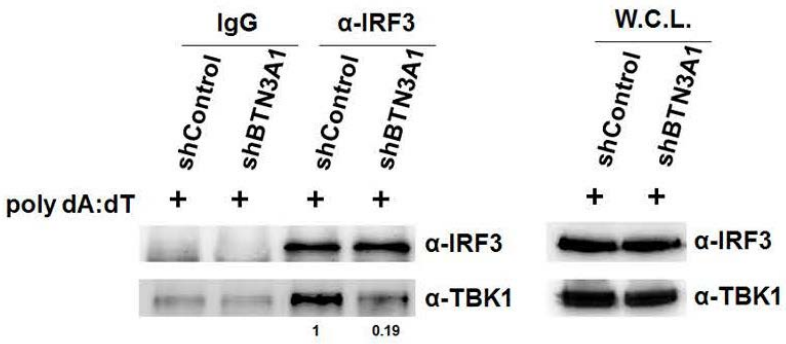
IgG
α-IRF3
W.C.L.
shControl
shBTN3A1
shControl
shBTN3A1
shControl
shBTN3A1
poly dA:dT
+
+
+
+
+
+
α-IRF3
α-TBK1
α-IRF3
α-TBK1
1
0.19

Figure 24. BTN3A1 mediates TBK1-IRF3 association

Immunoblot analysis (anti-IRF3 and anti-TBK1) of lysates from THP-1 cells treated with shControl or shBTN3A1 and stimulated for 3 hr with dsDNA, before (left) or after (right) immunoprecipitation with anti-IRF3.

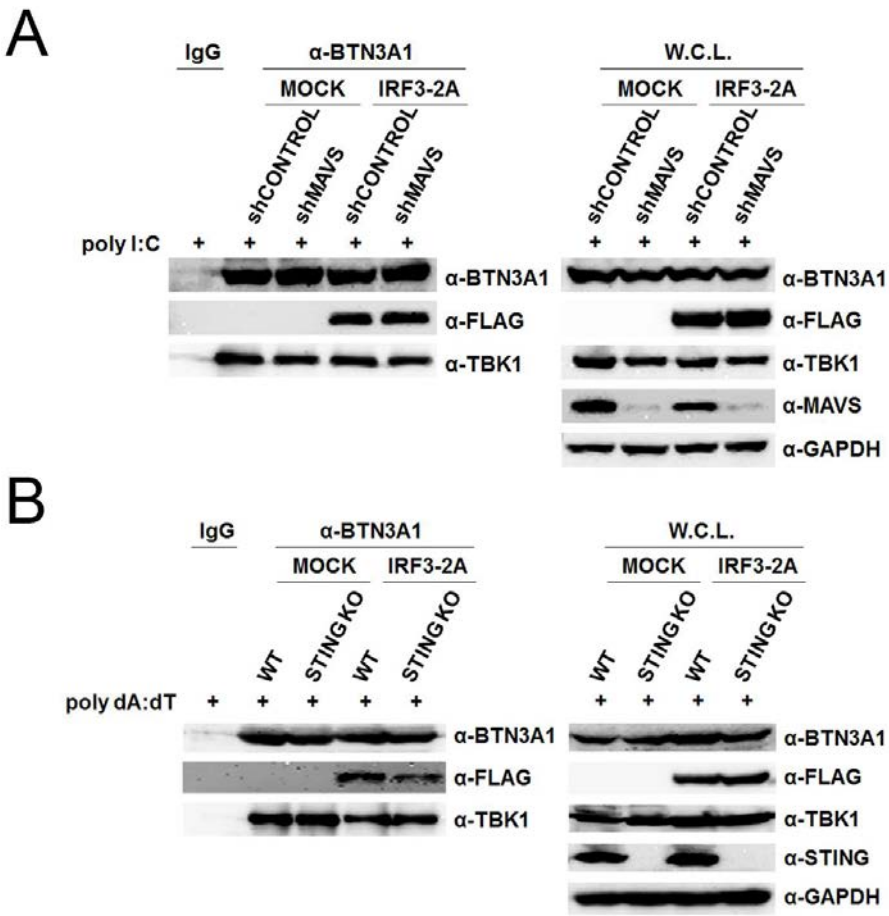
A
IgG
α-BTN3A1
W.C.L.
MOCK
IRF3-2A
MOCK
IRF3-2A
shCONTROL
shMAVS
shCONTROL
shMAVS
shCONTROL
shMAVS
shCONTROL
shMAVS
poly I:C
+ + + + +
+ + + + +
α-BTN3A1
α-FLAG
α-TBK1
α-BTN3A1
α-FLAG
α-TBK1
α-MAVS
α-GAPDH
B
IgG
α-BTN3A1
W.C.L.
MOCK
IRF3-2A
MOCK
IRF3-2A
WT
STING KO
WT
STING KO
WT
STING KO
WT
STING KO
poly dA:dT
+ + + + +
+ + + + +
α-BTN3A1
α-FLAG
α-TBK1
α-BTN3A1
α-FLAG
α-TBK1
α-STING
α-GAPDH

Figure 25. MAVS and STING are dispensable for the formation of BTN3A1-TBK1-IRF3 complex

(A) Immunoassay of extracts from transfected HEK293T cells treated with shControl or shMAVS and stimulated with poly I:C for 3 hr. (B) WT and STING KO cells were transfected with either mock or IRF3A-2A and stimulated with poly dA:dT for 3 hr. Cellular lysates were immunoprecipitated with anti-IgG or anti-BTN3A1 antibodies followed by immunoblotting with the indicated antibodies.

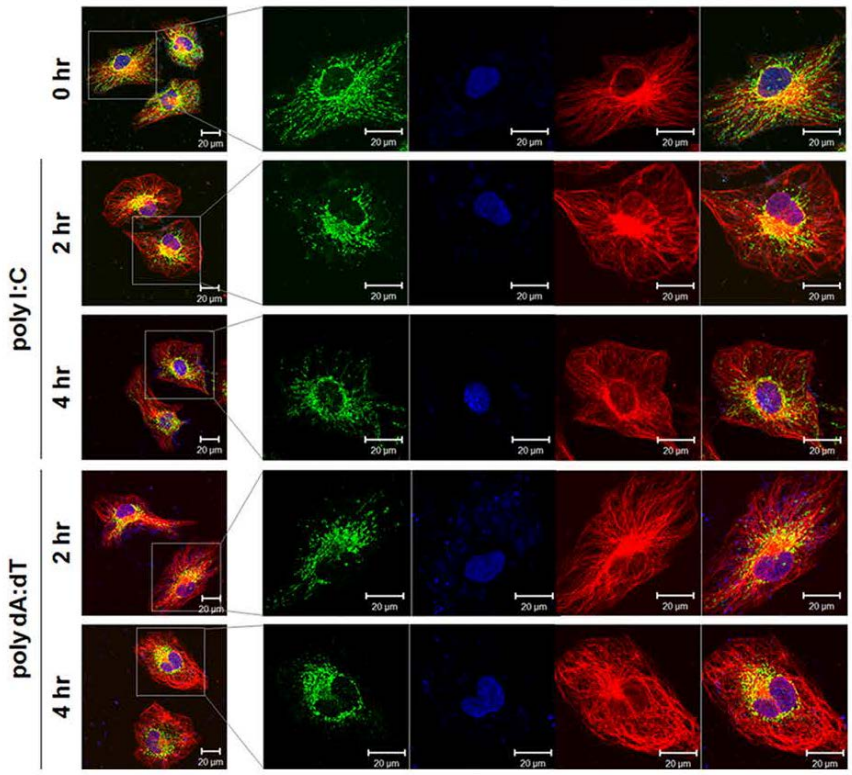
poly I:C
poly dA:dT
0 hr
2 hr
4 hr
2 hr
4 hr
20 μm

Figure 26. Movement of BTN3A1 in perinuclear region in response to nucleic acid stimulation

Confocal microscopic analysis of BTN3A1 (green) and α-Tubulin (red) in HeLa cells stimulated with poly I:C or poly dA:dT for the indicated durations. Nuclei were counterstained with DAPI (blue). Original magnification, 40x.

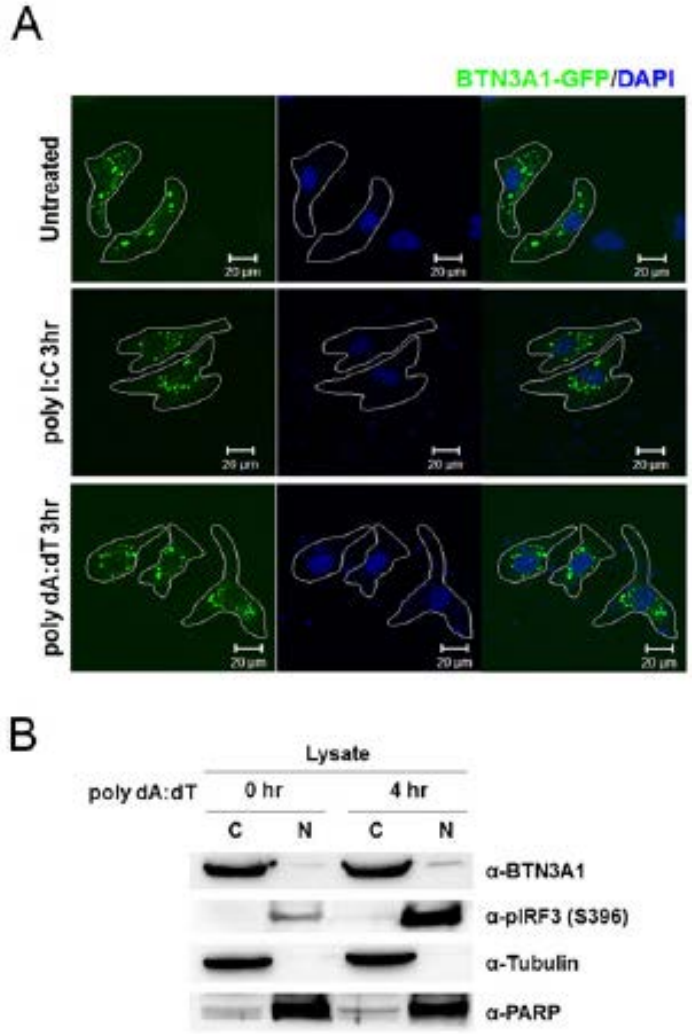
A
BTN3A1-GFP/DAPI
Untreated
poly I:C 3hr
poly dA:dT 3hr
20 μm
B
Lysate
poly dA:dT
0 hr
4 hr
C
N
C
N
α-BTN3A1
α-pIRF3 (S396)
α-Tubulin
α-PARP

Figure 27. Subcellular localization and perinuclear trafficking of BTN3A1

(A) Confocal microscopic analysis of BTN3A1-GFP in HeLa cells stimulated with poly I:C or poly dA:dT for 3 hr. Nuclei were counterstained with DAPI (Blue). Original magnification, 40x. (B) Immunoblotting for α-Tubulin, PARP, phosphoIRF3, and BTN3A1 in the cytosol (C) or nuclei (N) of THP-1 cells stimulated with poly dA:dT for 4 hr. Immunoblotting for phosphoIRF3 revealed dsDNA-induced activation.

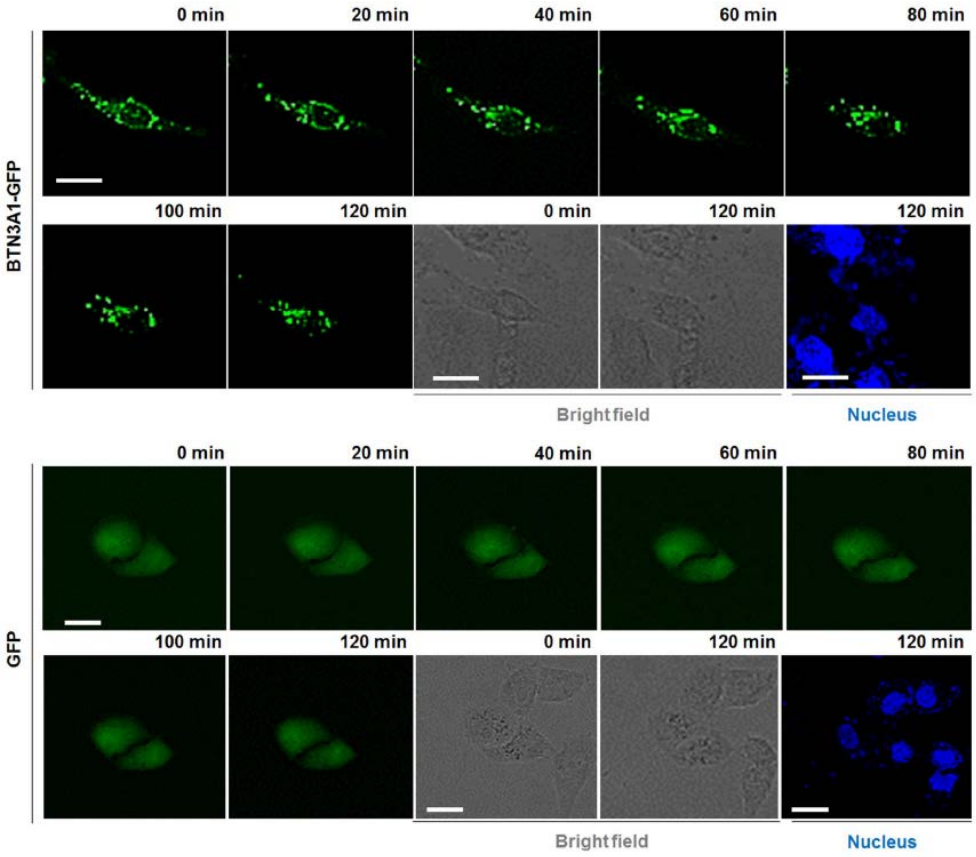
0 min
20 min
40 min
60 min
80 min
BTN3A1-GFP
100 min
120 min
0 min
120 min
120 min
Bright field
Nucleus
0 min
20 min
40 min
60 min
80 min
GFP
100 min
120 min
0 min
120 min
120 min
Bright field
Nucleus

Figure 28. BTN3A1 translocates to the perinuclear region in response to nucleic acid stimulation

Live cell imaging in HeLa cells transfected with BTN3A1-GFP followed by stimulation with poly dA:dT for 2 hr. Frames were captured every 20 min for total period of 120 min. Scale bar represents 30 μm.

4. Microtubule-Dependent Transport of BTN3A1 to the Perinuclear Region

Based on the observation that the activation of type I IFN signaling by nucleic acid promotes the spatial rearrangement of BTN3A1 and BTN3A1 colocalizes with tubulin, we asked whether microtubules control the subcellular localization of BTN3A1 upon nucleic acid stimulation. We examined the effect of microtubule depolymerization on the localization of BTN3A1 in nucleic acid-stimulated cells. Colchicine induced microtubule depolymerization, as visualized by immunostaining with anti-tubulin antibody. Accordingly, the localization of BTN3A1 to the perinuclear region was impaired in nucleic acid-stimulated cells (Figure 29). Colchicine-induced depolymerization of microtubules inhibited IFN-β production in response to dsDNA in a dose-dependent manner. Furthermore, to confirm that the effects on IFN-β production were due to microtubule disruption rather than a non-specific effect of colchicine, we utilized nocodazole, another microtubule-depolymerizing reagent, and obtained essentially the same results (Figure 30 A and B). Microtubule motors traffic vesicular cargo along microtubule tracks, with the dynein motor mediating retrograde movement and the kinesin motor mediating anterograde movement. We investigated the possible involvement of microtubule motors in the movement of BTN3A1 toward the perinuclear region. Treatment of cells with the dynein inhibitor ciliobrevin D caused a significant decrease in the level of IFN-β in response to dsDNA (Figure 30 A and B), whereas treatment of the cells with the kinesin inhibitor SB743921 did not influence IFN-β production after stimulation with poly I:C or poly dA:dT (Figure 30C). Neither colchicine, nocodazole nor ciliobrevin D significantly affected the production of TNF-α in

response to poly dA:dT, suggesting that these drugs did not affect the NF-κB-dependent induction of proinflammatory cytokines (Figure 30B). The treatment of cells with ciliobrevin D suppressed the phosphorylation of IRF3 but not TBK1 (Figure 31). The inhibition of dynein by ciliobrevin D did not interfere with the nuclear translocation of phosphoIRF3 (Figure 31). These data suggest that the dynein-mediated retrograde movement of BTN3A1 to the perinuclear region is required for triggering type I IFN signaling and that BTN3A1 functions downstream of TBK1 phosphorylation and upstream of IRF3 phosphorylation.

Intriguingly, BTN3A1 appears to be constitutively complexed with TBK1, regardless of nucleic acid challenge or microtubule integrity. The BTN3A1-IRF3 interactions, however, were reduced upon disrupting microtubule integrity by drug treatment (Figure 32A). Moreover, the treatment of cells with colchicine interfered with the interaction of TBK1 and IRF3 and subsequently suppressed the phosphorylation of IRF3 (Figure 32B). These findings indicate that BTN3A1 plays a role in trafficking TBK1 to the perinuclear region where BTN3A1 mediates the interaction between TBK1 and IRF3.

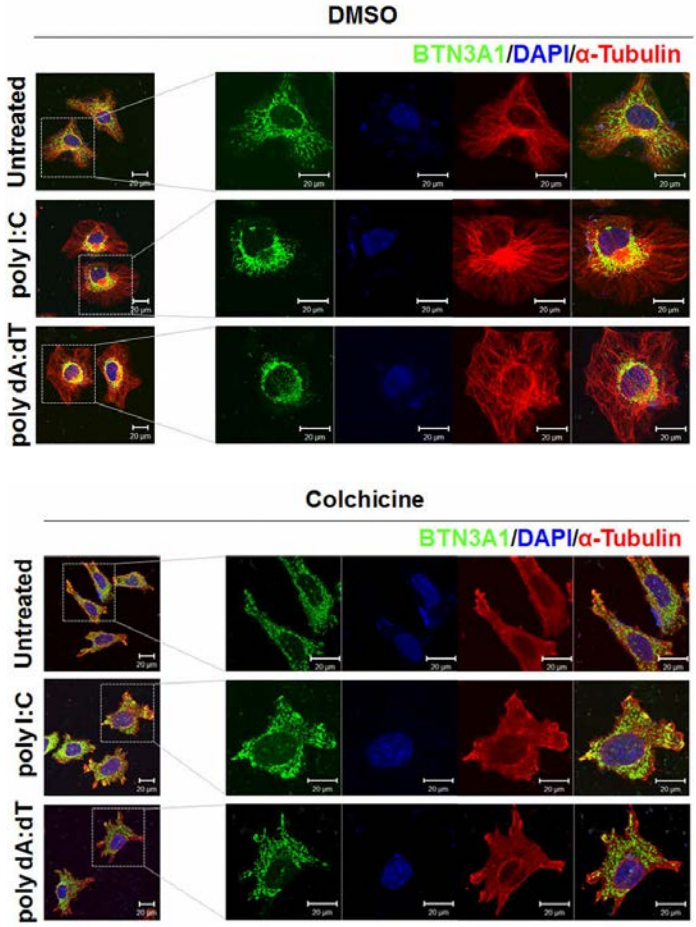
DMSO
BTN3A1/DAPI/α-Tubulin
Untreated
poly I:C
poly dA:dT
Colchicine
BTN3A1/DAPI/α-Tubulin
Untreated
poly I:C
poly dA:dT

Figure 29. Microtubule dependent movement of BTN3A1

Immunocytochemistry to reveal the subcellular location of BTN3A1 (green) and α-Tubulin (red) in HeLa cells pretreated with DMSO or colchicine (10 μM) and then left unstimulated or stimulated for 3 hr with poly I:C or poly dA:dT. DAPI serves as a nuclear marker. Original magnification, 40x.

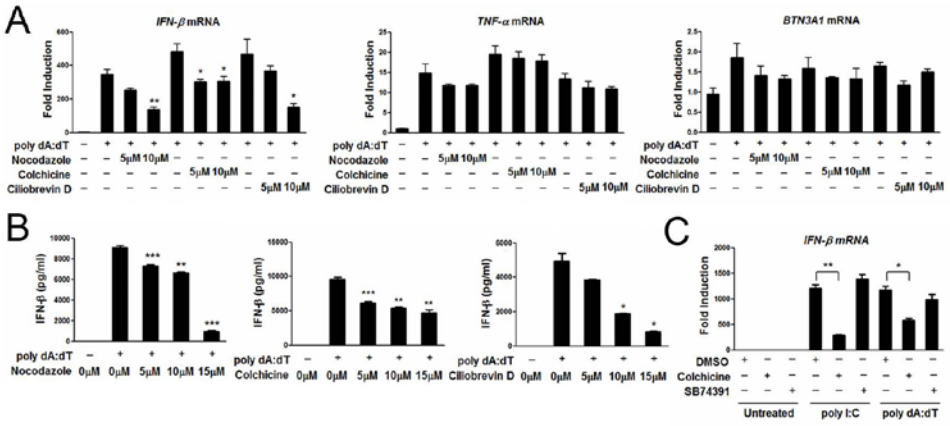
A
IFN-β mRNA
TNF-α mRNA
BTN3A1 mRNA
Fold Induction
poly dA:dT
Nocodazole
Colchicine
Ciliobrevin D
5μM 10μM
B
IFN-β (pg/ml)
poly dA:dT
Nocodazole 0μM 0μM 5μM 10μM 15μM
Colchicine 0μM 0μM 5μM 10μM 15μM
Ciliobrevin D 0μM 0μM 5μM 10μM 15μM
C
IFN-β mRNA
Fold Induction
DMSO
Colchicine
SB74391
Untreated
poly I:C
poly dA:dT

Figure 30. Microtubules are required for type I IFN signaling

(A) qRT-PCR analysis of IFN-β and TNF-α mRNA in THP-1 cells pretreated with increasing doses of nocodazole, colchicine or ciliobrevin D and then left unstimulated (-) or stimulated for 4 hr with poly dA:dT (+). (B) ELISA for IFN-β in the culture supernatants of THP-1 cells pretreated with increasing doses of nocodazole, colchicine or ciliobrevin D for 1 hr before stimulation with poly dA:dT (+), followed by analysis 6 hr later. (C) qRT-PCR analysis of IFN-β mRNA expression in DMSO-treated, 10 μM colchicine-treated or 10 μM SB74391 (a kinesin-specific inhibitor)-treated THP-1 cells in the presence of poly I:C or poly dA:dT for 4 hr. * $P<0.05$, ** $P<0.01$ and *** $P<0.001$ versus cells treated with DMSO (Student ' s t-test). The data are representative of three independent experiments.

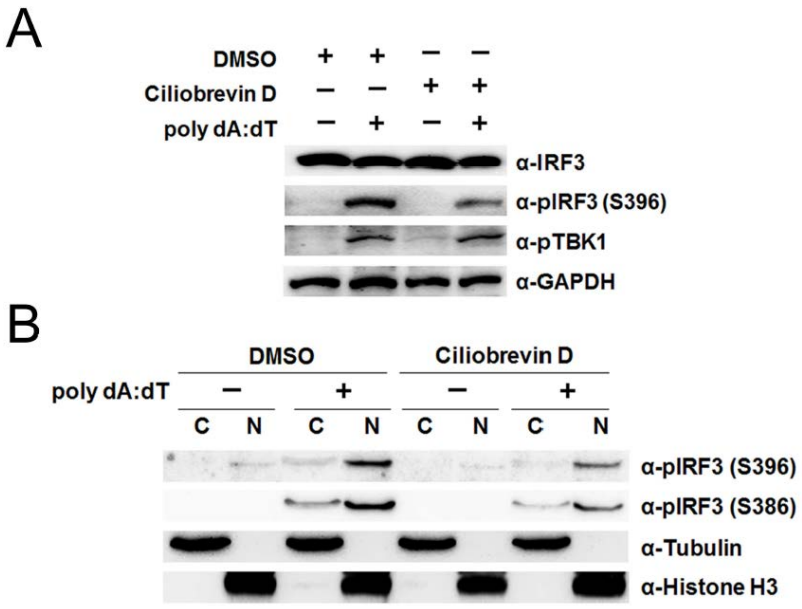
A
DMSO + + − −
Ciliobrevin D − − + +
poly dA:dT − + − +
α-IRF3
α-pIRF3 (S396)
α-pTBK1
α-GAPDH
B
DMSO
Ciliobrevin D
poly dA:dT − + − +
C N C N C N C N
α-pIRF3 (S396)
α-pIRF3 (S386)
α-Tubulin
α-Histone H3

Figure 31. Dynein is involved in the induction of type I IFN signaling

(A) Immunoblot analysis of extracts from THP-1 cells pretreated with DMSO or 10 μM ciliobrevin D, followed by stimulation with poly dA:dT for 4 hr. (B) Immunoblot of α-Tubulin, Histone H3, and phosphoIRF3 in the cytosolic (C) and nuclear (N) fraction of DMSO or 10 μM ciliobrevin D-treated THP-1 cells after stimulation with poly dA:dT for 4 hr.

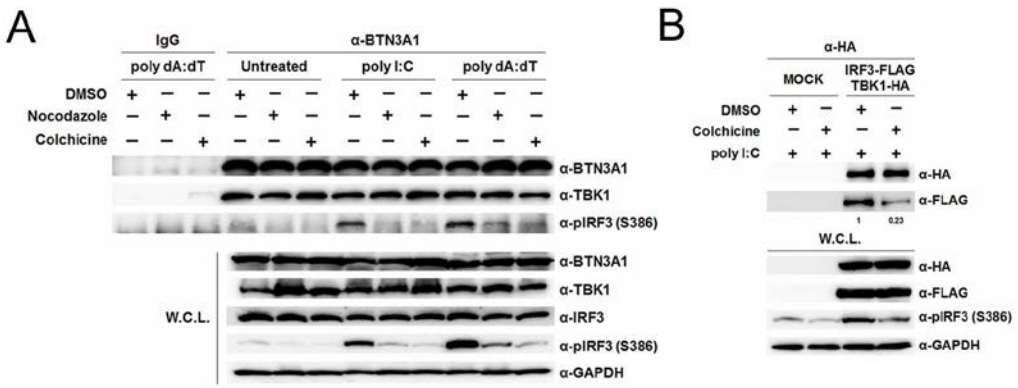
A
IgG
α-BTN3A1
poly dA:dT
Untreated
poly I:C
poly dA:dT
DMSO
Nocodazole
Colchicine
α-BTN3A1
α-TBK1
α-pIRF3 (S386)
W.C.L.
α-BTN3A1
α-TBK1
α-IRF3
α-pIRF3 (S386)
α-GAPDH
B
α-HA
MOCK
IRF3-FLAG
TBK1-HA
DMSO
Colchicine
poly I:C
α-HA
α-FLAG
1
0.23
W.C.L.
α-HA
α-FLAG
α-pIRF3 (S386)
α-GAPDH

Figure 32. Microtubule-dependent trafficking of BTN3A1 is critical to trigger type I IFN signaling

(A) Immunoprecipitation with anti-IgG or anti-BTN3A1 antibodies and immunoblotting with the indicated antibodies in THP-1 cells pretreated with DMSO, nocodazole or colchicine for 1 hr and then unstimulated or stimulated with poly I:C or poly dA:dT for 3 hr. (B) Immunoprecipitation and immunoblot analyses of extracts from HEK293T cells transfected with plasmids containing IRF3-FLAG and TBK-HA and then treated with DMSO or colchicine for 1 hr, followed by stimulation for 3 hr with poly I:C.

5. MAP4 is essential for type I IFN signaling by controlling the trafficking of BTN3A1

We addressed the question of what governs the trafficking of BTN3A1 in response to nucleic acids. To identify the novel interacting partners of BTN3A1, we performed co-immunoprecipitation followed by LC/MS analysis, which allowed the identification of microtubule associated protein 4 (MAP4) (Figure 33). Co-immunoprecipitation followed by immunoblot analysis revealed that BTN3A1 binds endogenous MAP4 (Figure 34A), confirming our LC/MS analysis results. We mapped the interacting domains of BTN3A1 and MAP4 using co-immunoprecipitation experiments. B30.2 domain of BTN3A1 alone could bind to MAP4, although the full-length BTN3A1 showed a stronger interaction with MAP4 (Figure 34B). We found that microtubule-binding domain of MAP4 is involved in the association with BTN3A1 (Figure 34C). To investigate whether MAP4 directly associates with type I IFN response in the nucleic acid-triggered immune response, we measured the effect of MAP4 on the induction of IFN-β. The shRNA-mediated knockdown of MAP4 led to the reduction of IFN-β production upon nucleic acid stimulation, including poly I:C and poly dA:dT, and SeV infection (Figure 35). Essentially the same results were obtained via a siRNA-mediated knockdown approach (Figure 36). Consistent with this result, the reduction of the mRNA of several interferon-stimulated genes (ISGs) such as IFITM1, IP-10, MxA, and OasL was observed in MAP4 depleted cells (Figure 37). IRF3 activation, as indicated by Ser386 phosphorylation, was also defective in nucleic acid stimulated or SeV infected shMAP4 cells (Figure 38A). Moreover, confocal microscopy analyses indicated that IRF3 is localized in the cytoplasm in unstimulated shControl cells but is redistributed predominantly to the nucleus

after nucleic acid stimulation. In shMAP4 cells, IRF3 was largely retained in the cytoplasm, even after nucleic acid stimulation (Figure 38B). Because MAP4 has been shown to regulate microtubule-based transport [43], we assessed whether MAP4 could affect the trafficking of BTN3A1 in response to nucleic acid stimulation. Knockdown of MAP4 inhibited the nucleic acid-induced retrograde movement of BTN3A1 to the perinuclear region (Figure 39). The strong association between endogenous BTN3A1 and IRF3 that was observed in shControl cells with nucleic acid stimulation was considerably diminished in shMAP4 cells (Figure 40). Next, we examined the specificity of MAP4 in type I IFN signaling. Since MAP2, MAP6, and TAU showed very low expression levels, we excluded them for further analysis (Figure 41A). siRNA-mediated depletion of MAP4 or other MAPs did not affect cell viability (Fig. 41 B-D). Among the other MAPs, only MAP4 appeared to be required for optimal expression level of IFN-β in response to RNA stimulation. Notable is that MAP7 might be a negative regulator in RNA-mediated type I IFN signaling (Figure 41E).

A

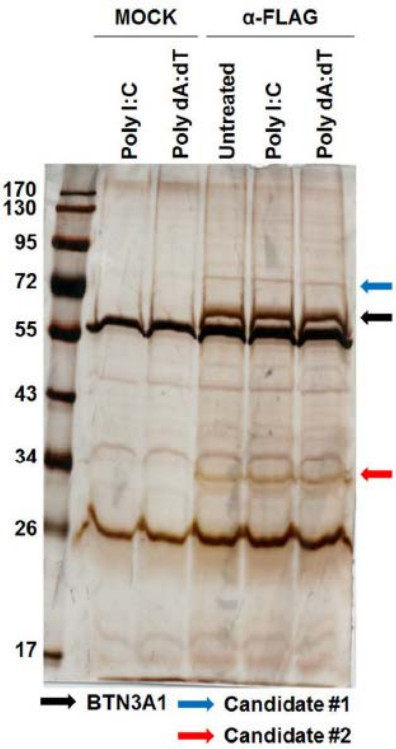

B

>MAP4 (Human) – 979aa from candidate #1

MADLSLADALTEPSPDIEGEIKRDFIATLEAEAFDDVVGETVGKTDYIPLLDVDEKTGNSESKKKPCSETSQ
IEDTPSSKPTLLANGGHGVEGSDTTGSPTEFLEEKMAYQEYPNSQNWPDTNFCFQPEQVVDPIQTDPFK
MYHDDDLADLVFPSSATADTSIFAGQNDPLKDSYGMSPCNTAVVPQGWSVEALNSPHSESFVSPEAVAE
PPQPTAVPLELAKEIEMASEERPPAQALEIMMGLKTTDMAPSKETEMALAKDMALATKTEVALAKDMESP
TKLDVTLAKDMQPSMESDMALVKDMELPTEKEVALVKDVRWPTETDVSSAKNVVLPTETEVAPAKDVTLL
KETERASPIKMDLAPSKDMGPPKENKKETERASPIKMDLAPSKDMGPPKENKIVPAKDLVLLSEIEVAQAN
DIISSTEISSAEKVALSSETEVALARDMTLPPETNVILTKDKALPLEAEVAPVKDMAQLPETEIAPAKDVAPS
TVKEVGLLKDMSPLSETEMALGKDVTPPPETEVVLIKNVCLPPEMEVALTEDQVPALKTEAPLAKDGVLTL
ANNVTPAKDVPPLSETEATPVPIKDMEIAQTQKGISEDSHLESLQDVGQSAAPTFMISPETVTGTGKKCSL
PAEEDSVLEKLGERKPCNSQPSELSSETSGIARPEEGRPVVSGTGNDITTPPNKELPPSPEKKTKPLATTQ
PAKTSTSKAKTQPTSLPKQPAPTTIGGLNKKPMSLASGLVPAAPPKRPAVASARPSILPSKDVKPKPIADAK
APEKRASPSKPASAPASRSGSKSTQTVAKTTTAAAVASTGPSSRSPSTLLPKKPTAIKTEGKPAEVKKMTA
KSVPADLSRPKSTSTSSMKKTTTLSGTAPAAGVVPSRVKATPMPSRPSTTPFIDKKPTSAKPSSTTPRLSR
LATNTSAPDLKNVRSKVGSTENIKHQPGGGRAKVEKKTEAAATTRKPESNAVTKTAGPIASAQKQPAGKV
QIVSKKVSYSHIQSKCGSKDNIKHVPGGGNVQIQNKKVDISKVSSKCGSKANIKHKPGGGDVKIESQKLNF
KEKAQAKVGSLDNVGHLPAGGAVKTEGGGSEAPLCPGPPAGEEPAISEAAPEAGAPTSASGLNGHPTLS
GGGDQREAQTLDSQIQETSI

Red : identified peptides by MS

>MAP4 (Human) – 979aa from candidate #2

MADLSLADALTEPSPDIEGEIKRDFIATLEAEAFDDVVGETVGKTDYIPLLDVDEKTGNSESKKKPCSETSQ
IEDTPSSKPTLLANGGHGVEGSDTTGSPTEFLEEKMAYQEYPNSQNWPDTNFCFQPEQVVDPIQTDPFK
MYHDDDLADLVFPSSATADTSIFAGQNDPLKDSYGMSPCNTAVVPQGWSVEALNSPHSESFVSPEAVAE
PPQPTAVPLELAKEIEMASEERPPAQALEIMMGLKTTDMAPSKETEMALAKDMALATKTEVALAKDMESP
TKLDVTLAKDMQPSMESDMALVKDMELPTEKEVALVKDVRWPTETDVSSAKNVVLPTETEVAPAKDVTLL
KETERASPIKMDLAPSKDMGPPKENKKETERASPIKMDLAPSKDMGPPKENKIVPAKDLVLLSEIEVAQAN
DIISSTEISSAEKVALSSETEVALARDMTLPPETNVILTKDKALPLEAEVAPVKDMAQLPETEIAPAKDVAPS
TVKEVGLLKDMSPLSETEMALGKDVTPPPETEVVLIKNVCLPPEMEVALTEDQVPALKTEAPLAKDGVLTL
ANNVTPAKDVPPLSETEATPVPIKDMEIAQTQKGISEDSHLESLQDVGQSAAPTFMISPETVTGTGKKCSL
PAEEDSVLEKLGERKPCNSQPSELSSETSGIARPEEGRPVVSGTGNDITTPPNKELPPSPEKKTKPLATTQ
PAKTSTSKAKTQPTSLPKQPAPTTIGGLNKKPMSLASGLVPAAPPKRPAVASARPSILPSKDVKPKPIADAK
APEKRASPSKPASAPASRSGSKSTQTVAKTTTAAAVASTGPSSRSPSTLLPKKPTAIKTEGKPAEVKKMTA
KSVPADLSRPKSTSTSSMKKTTTLSGTAPAAGVVPSRVKATPMPSRPSTTPFIDKKPTSAKPSSTTPRLSR
LATNTSAPDLKNVRSKVGSTENIKHQPGGGRAKVEKKTEAAATTRKPESNAVTKTAGPIASAQKQPAGKV
QIVSKKVSYSHIQSKCGSKDNIKHVPGGGNVQIQNKKVDISKVSSKCGSKANIKHKPGGGDVKIESQKLNF
KEKAQAKVGSLDNVGHLPAGGAVKTEGGGSEAPLCPGPPAGEEPAISEAAPEAGAPTSASGLNGHPTLS
GGGDQREAQTLDSQIQETSI

Red : identified peptides by MS

Figure 33. Identification of MAP4 as a BTN3A1 interacting partner

(A) Silver staining of FLAG-associated proteins purified with a FLAG antibody from HEK293T cells transfected with a mock or BTN3A1-FLAG and then stimulated with poly I:C or poly dA:dT for 3 hr. (B) Peptides identified by LC/MS spectrometry.

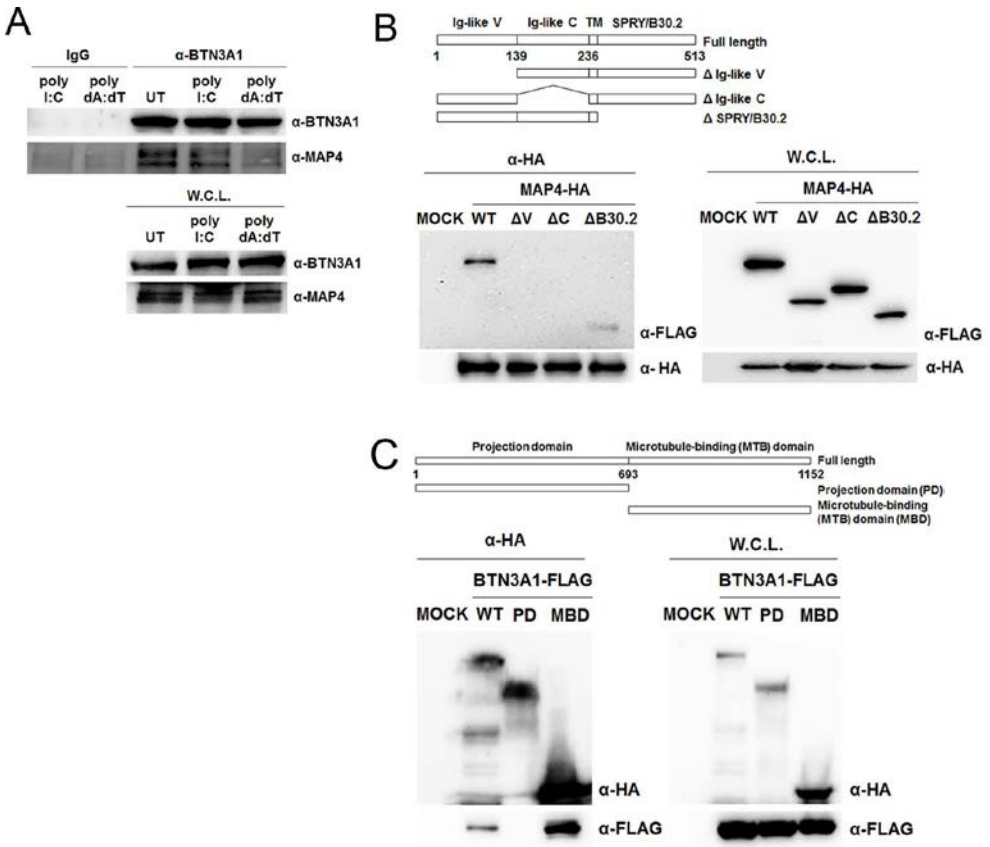
A
IgG
α-BTN3A1
poly I:C
poly dA:dT
UT
poly I:C
poly dA:dT
α-BTN3A1
α-MAP4
W.C.L.
UT
poly I:C
poly dA:dT
α-BTN3A1
α-MAP4
B
Ig-like V
Ig-like C
TM
SPRY/B30.2
Full length
1
139
236
513
Δ Ig-like V
Δ Ig-like C
Δ SPRY/B30.2
α-HA
MAP4-HA
MOCK WT ΔV ΔC ΔB30.2
α-FLAG
α- HA
W.C.L.
MAP4-HA
MOCK WT ΔV ΔC ΔB30.2
α-FLAG
α-HA
C
Projection domain
Microtubule-binding (MTB) domain
Full length
1
693
1152
Projection domain (PD)
Microtubule-binding (MTB) domain (MBD)
α-HA
BTN3A1-FLAG
MOCK WT PD MBD
α-HA
α-FLAG
W.C.L.
BTN3A1-FLAG
MOCK WT PD MBD
α-HA
α-FLAG

Figure 34. BTN3A1 interacts with MAP4

(A) Immunoassay of extracts from THP-1 cells untreated (UT) or treated with poly I:C or poly dA:dT for 3 hr, followed by immunoprecipitation with anti-IgG or anti-BTN3A1 antibodies and immunoblot analysis with anti-BTN3A1 and anti-MAP4. (B and C) Schematic representations of BTN3A1 (B) and MAP4 derivatives (C). Immunoprecipitation analysis of HEK293T cells co-transfected with the indicated combinations of expression plasmids, followed by immunoblotting with anti-HA.

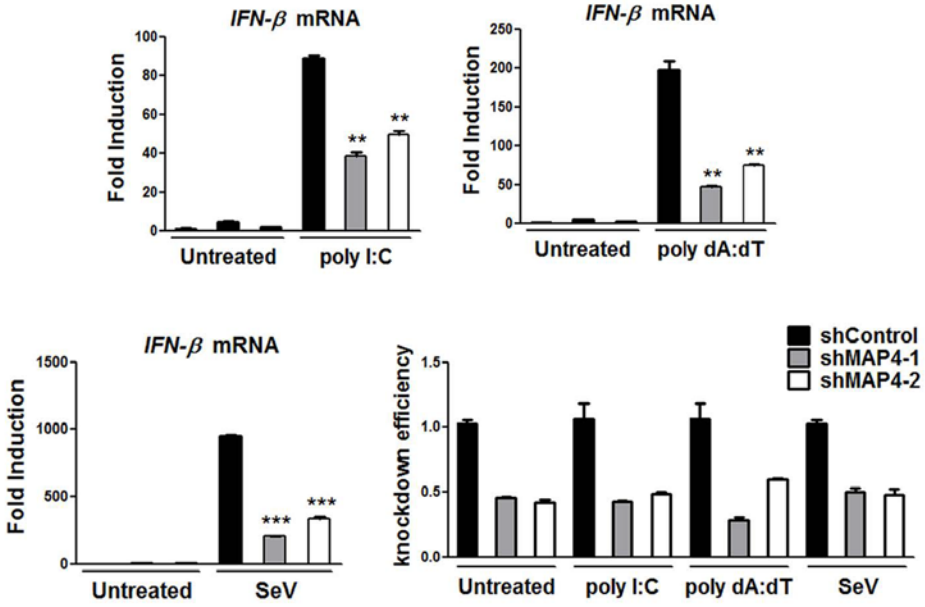
IFN-β mRNA
Fold Induction
100
80
60
40
20
0
**
**
Untreated
poly I:C
IFN-β mRNA
Fold Induction
250
200
150
100
50
0
**
**
Untreated
poly dA:dT
IFN-β mRNA
Fold Induction
1500
1000
500
0
***
***
Untreated
SeV
knockdown efficiency
1.5
1.0
0.5
0.0
shControl
shMAP4-1
shMAP4-2
Untreated
poly I:C
poly dA:dT
SeV

Figure 35. MAP4 is critical for type I IFN signaling

qRT- PCR analysis of IFN-β and MAP4 mRNA in THP-1 cells transfected with shControl or shMAP4 and left untreated (UT) or stimulated with poly I:C or poly dA:dT, or infected with SeV for 4 hr. ** $P<0.01$ and *** $P<0.001$ versus cells transfected with shcontrol (Student ' s t-test). Data are representative of three independent experiments.

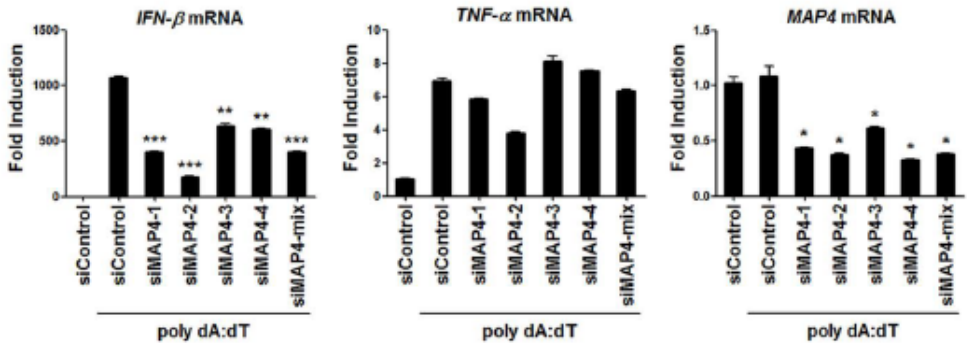
IFN-β mRNA
Fold Induction
1500
1000
500
0
***
***
**
**
***
siControl
siControl
siMAP4-1
siMAP4-2
siMAP4-3
siMAP4-4
siMAP4-mix
poly dA:dT
TNF-α mRNA
Fold Induction
10
8
6
4
2
0
siControl
siControl
siMAP4-1
siMAP4-2
siMAP4-3
siMAP4-4
siMAP4-mix
poly dA:dT
MAP4 mRNA
Fold Induction
1.5
1.0
0.5
0.0
*
*
*
*
*
siControl
siControl
siMAP4-1
siMAP4-2
siMAP4-3
siMAP4-4
siMAP4-mix
poly dA:dT

Figure 36. MAP4 is necessary for type I IFN signaling

qRT-PCR analysis of IFN-β, TNF-α and MAP4 mRNA in THP-1 cells treated with control siRNA or siRNAs targeting MAP4 and then stimulated with poly dA:dT for 4 hr. * $P<0.05$, ** $P<0.01$ and *** $P<0.001$ versus cells transfected with control siRNA (Student's t-test). Data are representative of three independent experiments.

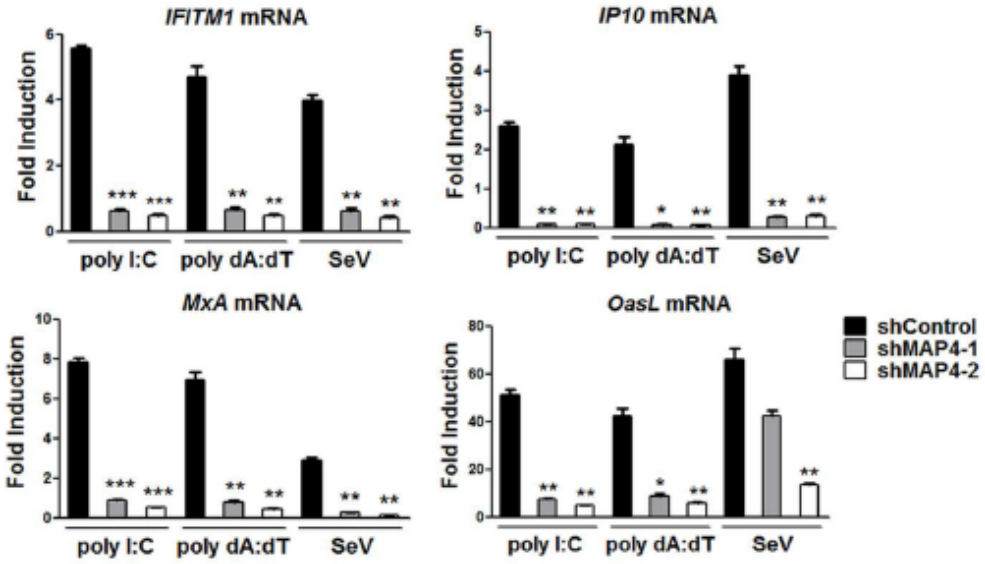
IFITM1 mRNA
IP10 mRNA
MxA mRNA
OasL mRNA
Fold Induction
poly I:C
poly dA:dT
SeV
shControl
shMAP4-1
shMAP4-2

Figure 37. MAP4 is indispensable for induction of IFN-stimulatory genes

qRT-PCR analysis of IFITM1, IP10, MxA, and OasL mRNA in THP-1 cells transfected with shControl or shMAP4 and then stimulated with poly I:C or poly dA:dT or infected with SeV for 6 hr. * $P<0.05$, ** $P<0.01$ and *** $P<0.001$ versus cells transfected with control shRNA (Student's t-test). Data are representative of three independent experiments.

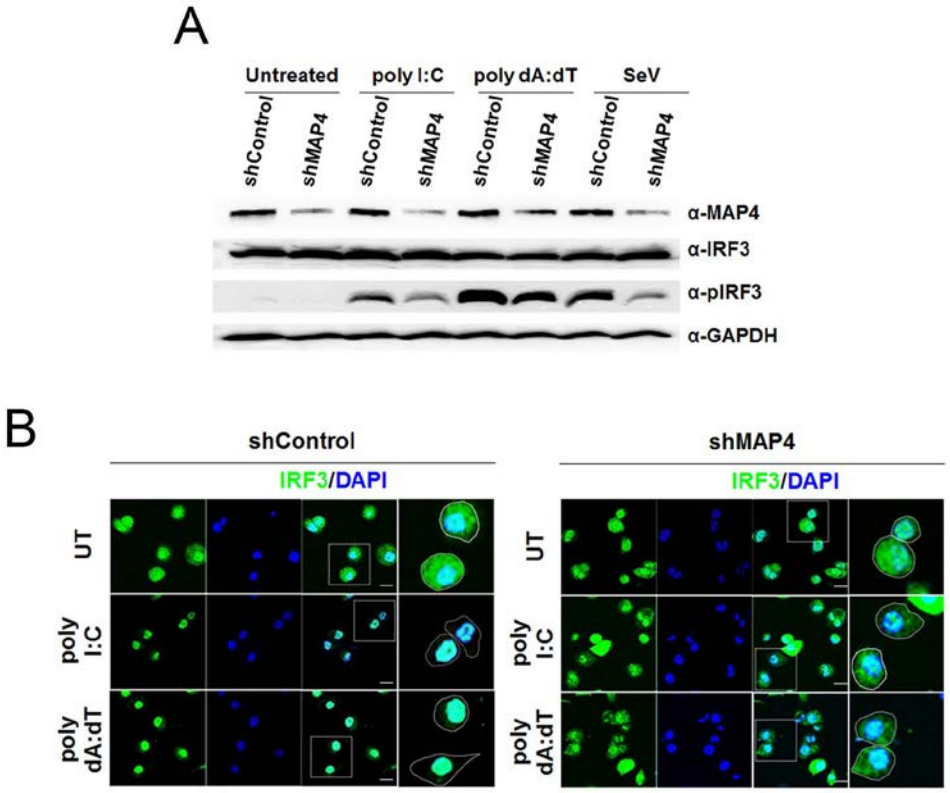
A
Untreated
poly I:C
poly dA:dT
SeV
shControl
shMAP4
shControl
shMAP4
shControl
shMAP4
shControl
shMAP4
α-MAP4
α-IRF3
α-pIRF3
α-GAPDH
B
shControl
shMAP4
IRF3/DAPI
IRF3/DAPI
UT
poly I:C
poly dA:dT
UT
poly I:C
poly dA:dT

Figure 38. MAP4 controls phosphorylation and nuclear translocation of IRF3

(A) Immunoblot analysis of extracts from THP-1 cells treated as described in D. (B) Confocal microscopy examining the nuclear localization of IRF3 in unstimulated, poly I:C or poly dA:dT stimulated THP1 cells pretreated with shControl or shMAP4. The scale bar represents 20 μm.

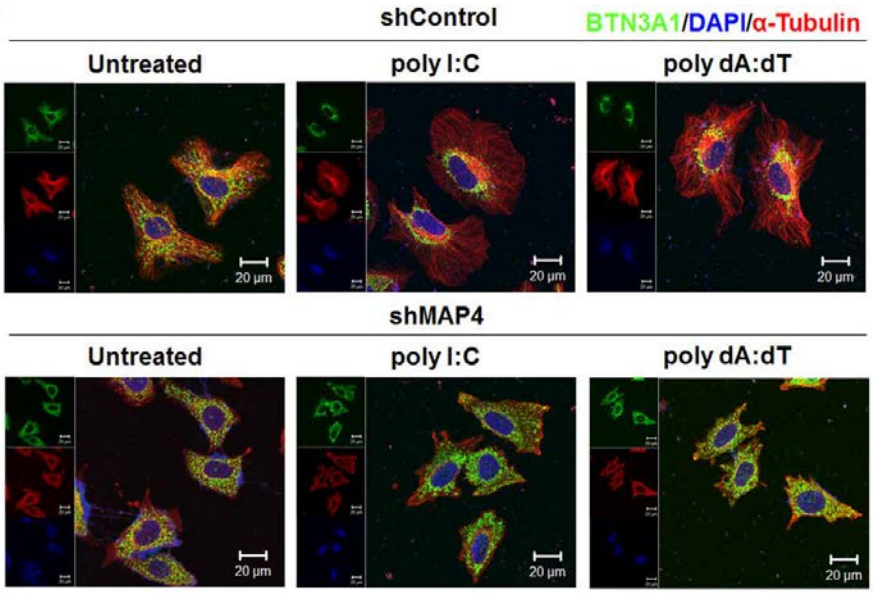
shControl
BTN3A1/DAPI/α-Tubulin
Untreated
poly I:C
poly dA:dT
20 μm
shMAP4
Untreated
poly I:C
poly dA:dT
20 μm

Figure 39. MAP4 governs the subcellular trafficking of BTN3A1

Confocal microscopic images of BTN3A1 (green) and α-Tubulin (red) in HeLa cells transfected with shControl or shRNA targeting MAP4 (shMAP4) and then left untreated or stimulated with poly I:C or poly dA:dT for 3 hr. DAPI was used to label nuclei. Original magnification, 40x.

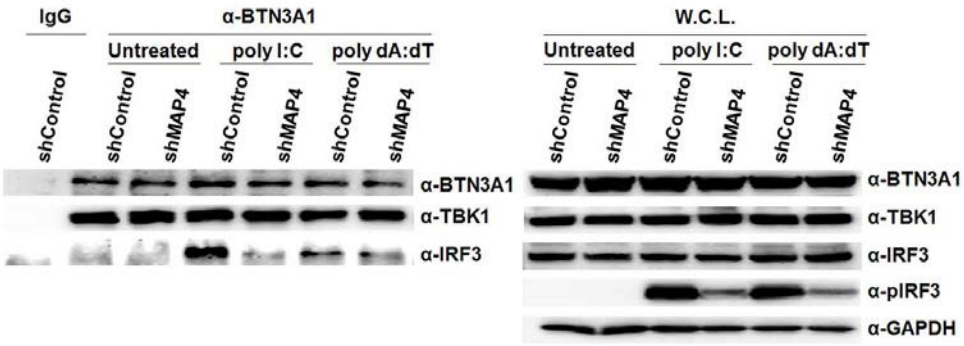
IgG
α-BTN3A1
Untreated
poly I:C
poly dA:dT
shControl
shMAP4
shControl
shMAP4
shControl
shMAP4
shControl
α-BTN3A1
α-TBK1
α-IRF3
W.C.L.
Untreated
poly I:C
poly dA:dT
shControl
shMAP4
shControl
shMAP4
shControl
shMAP4
α-BTN3A1
α-TBK1
α-IRF3
α-pIRF3
α-GAPDH

Figure 40. MAP4 is required for interaction of BTN3A1 with IRF3

Immunoassay of extracts from THP-1 cells treated with shControl or shMAP4 and stimulated with poly I:C or poly dA:dT for 3 hr, followed by immunoprecipitation with anti-IgG or anti-BTN3A1 antibodies and immunoblot analysis with the indicated antibodies.

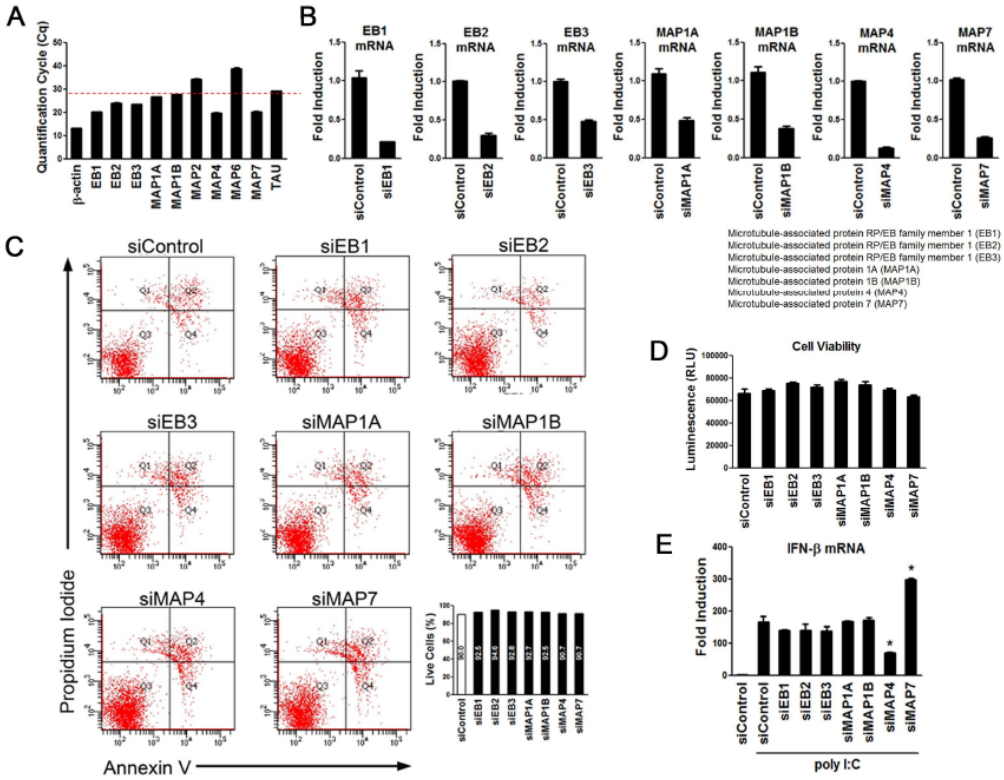
A
Quantification Cycle (Cq)
β-actin
EB1
EB2
EB3
MAP1A
MAP1B
MAP2
MAP4
MAP6
MAP7
TAU
B
EB1 mRNA
EB2 mRNA
EB3 mRNA
MAP1A mRNA
MAP1B mRNA
MAP4 mRNA
MAP7 mRNA
Fold Induction
siControl
siEB1
siEB2
siEB3
siMAP1A
siMAP1B
siMAP4
siMAP7
Microtubule-associated protein RP/EB family member 1 (EB1)
Microtubule-associated protein RP/EB family member 1 (EB2)
Microtubule-associated protein RP/EB family member 1 (EB3)
Microtubule-associated protein 1A (MAP1A)
Microtubule-associated protein 1B (MAP1B)
Microtubule-associated protein 4 (MAP4)
Microtubule-associated protein 7 (MAP7)
C
siControl
siEB1
siEB2
siEB3
siMAP1A
siMAP1B
siMAP4
siMAP7
Propidium Iodide
Annexin V
Q1
Q2
Q3
Q4
Live Cells (%)
90.0
82.5
84.6
83.8
82.7
82.5
80.7
80.7
D
Cell Viability
Luminescence (RLU)
E
IFN-β mRNA
Fold Induction
poly I:C

Figure 41. Specificity of MAP4 in type I IFN signaling

(A) qRT-PCR analysis of expression of various microtubule associated genes in HeLa cells. (B) siRNA-mediated knockdown ofEB1, EB2, EB3, MAP1A, MAP1B, MAP4 and MAP7 in HeLa cells. Knockdown efficiency was measured by qRT-PCR. (C) Evaluation of apoptosis by Annexin V-FITC and PI dual staining assay and flow cytometer analysis after siRNA treatment for 3 days. (D) Viability analysis of the indicated siRNA-transfected HeLa cells through measuring intracellular ATP level. (E) qRT-PCR analysis of IFN-β expression in HeLa cells treated with the indicated siRNAs and then stimulated with poly I:C for 4 hr. *P<0.05 versus cells transfected with control siRNA (Student's t-test). Data are representative of three independent experiments.

6. BTN3A1 interacts with dynein for trafficking to the perinuclear region

Next, we explored the functional role of MAP4 in mediating BTN3A1 trafficking in response to nucleic acids. MAP proteins compete with motor proteins for microtubule binding [44, 45], and the phosphorylation of MAPs induces the detachment of MAPs from microtubules [46, 47]. We observed that the phosphorylation of MAP4 occurs following nucleic acid stimulation and peaked at 3 hr of incubation (Figure 42A). Immunofluorescence staining showed that in the resting state, MAP4 is evenly dispersed throughout the cytoplasm, but MAP4 was found in small punctate aggregates after nucleic acid challenge, which could imply that it undergoes a spatial redistribution upon nucleic acid stimulation (Figure 42B). To test if TBK1 phosphorylates MAP4 to drive disassociation of MAP4 from microtubules, we silenced TBK1 using siRNA. Knockdown of TBK1 did not affect phosphorylation level of MAP4 but substantially decreased pIRF3 level, suggesting that MAP4 is not a substrate for TBK1-mediated phosphorylation (Figure 42C). Interestingly, we found that both dynein intermediate chain (DYNC) 1/1 and 1/2 interact with BTN3A1 in both the exogenously and the endogenously expressed proteins, and their interaction increased upon treatment with nucleic acid (Figure 43 A and B). These results support the notion that BTN3A1 moves to perinuclear region through dynein upon nucleic acid stimulation.

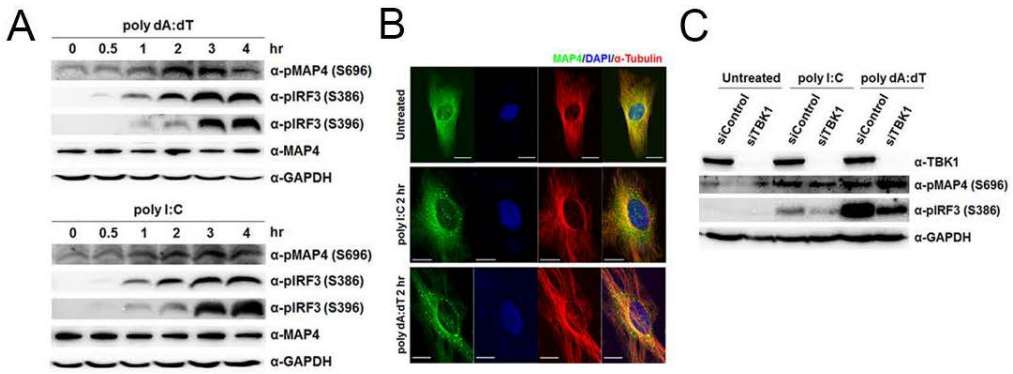
A
poly dA:dT
0 0.5 1 2 3 4 hr
α-pMAP4 (S696)
α-pIRF3 (S386)
α-pIRF3 (S396)
α-MAP4
α-GAPDH
poly I:C
0 0.5 1 2 3 4 hr
α-pMAP4 (S696)
α-pIRF3 (S386)
α-pIRF3 (S396)
α-MAP4
α-GAPDH
B
MAP4/DAPI/α-Tubulin
Untreated
poly I:C 2 hr
poly dA:dT 2 hr
C
Untreated
poly I:C
poly dA:dT
siControl
siTBK1
siControl
siTBK1
siControl
siTBK1
α-TBK1
α-pMAP4 (S696)
α-pIRF3 (S386)
α-GAPDH

Figure 42. Phosphorylation of MAP4 causes its dissociation from microtubules

(A) Immunoblot analysis of total and phosphorylated MAP4 as well as phosphorylated IRF3 as an indicator of nucleic acid-mediated activation in THP-1 cells stimulated with poly I:C or poly dA:dT for the indicated duration. (B) Confocal microscopic analysis of MAP4 (green) and α-Tubulin (red) in HeLa cells transfected with poly I:C or poly dA:dT for 2 hr. The scale bar represents 20 μm. (C) Immunoblot analysis of phosphorylation of MAP4 and IRF3 in siControl and siTBK1 cells after poly I:C or poly dA:dT stimulation.

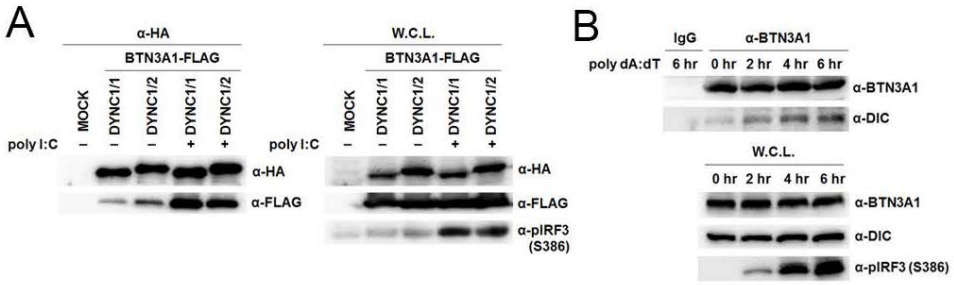
A
α-HA
BTN3A1-FLAG
MOCK
DYNC1/1
DYNC1/2
DYNC1/1
DYNC1/2
poly I:C
- - + +
α-HA
α-FLAG
W.C.L.
BTN3A1-FLAG
MOCK
DYNC1/1
DYNC1/2
DYNC1/1
DYNC1/2
poly I:C
- + + + +
α-HA
α-FLAG
α-pIRF3 (S386)
B
IgG
α-BTN3A1
poly dA:dT
6 hr
0 hr 2 hr 4 hr 6 hr
α-BTN3A1
α-DIC
W.C.L.
0 hr 2 hr 4 hr 6 hr
α-BTN3A1
α-DIC
α-pIRF3 (S386)

Figure 43. Nucleic acid stimulation leads to the interaction of BTN3A1 with dynein

(A) Immunoprecipitation analysis of HEK293T cells co-transfected with the indicated combinations of expression plasmids, followed by immunoblotting with anti-HA. DYNC denotes dynein intermediate chain. (B) Immunoprecipitation with anti-IgG or anti-BTN3A1 antibodies followed by immunoblot analysis for BTN3A1 and dynein in THP-1 cells treated with poly dA:dT for the indicated time.

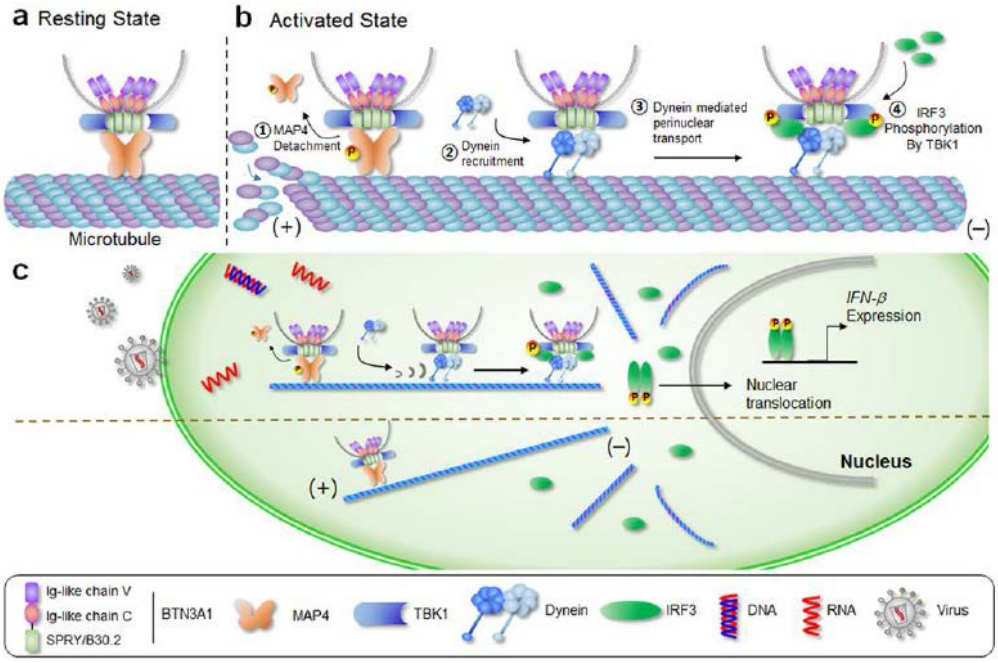

Figure 44. Roles for BTN3A1 and MAP4 in regulating type I IFN signaling

IV. DISCUSSION

Our study suggests a critical role for MAP4-regulated spatial arrangement of BTN3A1 in the activation of the TBK1/IRF3 signaling axis triggered by cytoplasmic RNA and DNA. In the resting state, BTN3A1 associates with TBK1, and the BTN3A1-TBK1 complex binds to MAP4 on microtubules. Upon nucleic acid stimulation, MAP4 is phosphorylated and released from the microtubules, thereby ensuring its availability for binding to the motor protein dynein. The BTN3A1-TBK1 complex then moves along microtubules to the perinuclear region where TBK1 phosphorylates IRF3, leading to the nuclear translocation of IRF3 and the induction of type I interferons (Figure 44).

To date, identified regulators of the type I IFN pathway have been shown to control sensors or adaptors upstream of the TBK1-IRF3 signaling axis in the nucleic acid mediated innate immune response [48-51]. These regulators are specific to a particular signaling pathway for certain types of nucleic acids. Nucleic acids from pathogens are detected by PRRs, including TLRs, RLRs, and cytosolic DNA sensors [4, 52]. Although nucleic acids in the endosome are recognized by TLRs and those in the cytosol are detected by RLRs or DNA sensors, all receptors require the TBK1-IRF3 axis to induce type I IFN signaling [52]. We found that BTN3A1 is required for the TBK1-mediated phosphorylation of IRF3, a downstream event in nucleic acid sensing for antiviral defense. Because TBK1 is a central node of the regulatory network required to trigger innate immune responses against various types of nucleic acids, BTN3A1 could serve as a master regulator of type I IFN signaling elicited by both DNA and

RNA virus infection. This is consistent with the finding that the depletion of either BTN3A1 or its regulator MAP4 abrogated the activation of the type I IFN response. Notably, we found that BTN3A1 controls the TBK-IRF3 axis activated by viral nucleic acids in the cytosol but not in the endosome, suggesting that sensing cytosolic nucleic acids drives BTN3A1 toward a functional form to initiate regulation.

Few reports have described a link between microtubules and innate immunity. Microtubules mediate the activation of the NLRP3 inflammasome by regulating the arrangement of mitochondria [53]. Chiang and colleagues characterized the microtubule-dependent sensing of nucleic acids through GEF-H1; they found that microtubule networks were essential for the GEF-H1-controlled recognition of viral RNA and synthetic dsRNAs in macrophages [38]. Our study showed that MAP4 regulates the dynein-based transport of BTN3A1 to the perinuclear region. Motor proteins and MAPs compete for the same binding sites on tubulin [44], and the phosphorylation of MAPs decreases their binding to tubulin [54]. In light of the results of previous reports and our observations, it is likely that cells initiate type I IFN signaling in response to nucleic acid stimuli by replacing MAP4 with dynein for binding to microtubules, which allows BTN3A1 to recruit TBK1 to the perinuclear region. However, at present, it is unclear how MAP4 is phosphorylated upon nucleic acid stimulation.

The transport of signaling components to the perinuclear region appears to be an important process in triggering type I IFN signaling. Previous studies have suggested that STING activation includes its trafficking from the ER to vesicles in the perinuclear region via the Golgi apparatus [16], although how innate immune signaling and STING trafficking are coordinated remains

unknown. The importance of the regulated trafficking of signaling molecules is underscored by the findings that Shigella inhibits STING signaling by blocking its translocation from the ER to ERGIC and that the ERGIC/Golgi trafficking mechanism of STING is deregulated in genetic autoinflammatory diseases [55]. Our work also demonstrated that the transport of BTN3A1-mediated TBK1 to the perinuclear region is critical for the induction of IFN-β gene expression in response to nucleic acid stimulation. The complex containing BTN3A1, TBK1 and IRF3 in the perinuclear region might involve a yet-to-be-identified compartmentalization wherein BTN3A1 acts as an adaptor molecule for the rapid and effective activation of type I IFN signaling. Our findings provide a spatiotemporal model for IRF3 activation and could lead to novel therapeutic strategies for nucleic acid-mediated inflammatory diseases.

V. EXPERIMENTAL PROCEDURES

Reagents and Antibodies

Poly I:C, poly dA:dT, LPS, nocodazole, colchicine, and human anti-FLAG antibody were purchased from Sigma; c-di-GMP and c-di-AMP were obtained from Invivogen; and cytoplasmic dynein inhibitor, ciliobrevin D, was obtained from Merck. Human anti-IRF3, PARP and SB743921 were from Santa Cruz; anti-TBK1, phospho-IRF3 (S396), phospho-TBK1, and STING were from Cell Signaling; anti-BTN3A1, phospho-IRF3 (S386), MAVS, IKK ε, Histone H3 and MAP4 were from Abcam; anti-GAPDH and α-tubulin were from Ab Frontier; and anti-HA was from Covance.

Cells and Viruses

HEK293T and HeLa cells were cultured in DMEM (Dulbecco's modified Eagle's medium) supplemented with 10% FBS (Thermo) in a 5% CO_2 incubator. THP-1 cells were maintained in RPMI medium containing 10% FBS and were treated with 100 nM PMA to induce differentiation. Peripheral blood mononuclear cells (PBMCs) were obtained from human blood by density gradient centrifugation using Ficoll-Paque Plus (Amersham Healthcare, Aylesbury, UK). Monocytes were isolated from PBMCs using a magnetic bead-based positive selection kit (IMag) and an anti-human CD14 antibody (BD Bioscience). To generate monocyte-derived macrophages (MDMs), CD14-positive cells were treated with human recombinant interleukin-4 (hrIL-4; R&D Systems) and human recombinant

granulocyte-macrophage colony stimulating factor (hrGM-CSF; R&D Systems) for 5 days. All experiments involving human blood were approved by the Institutional Review Board of Seoul National University (SNUIRB No. E1304-001-023).

HSV-1 virus was propagated on Vero cells. Viral stocks were prepared by infecting Vero cells at a multiplicity of infection (MOI) of 0.01. The infected cells were incubated at 37℃ for 48 hr. After three freeze-thaw cycles, cell debris was removed by centrifugation, and the supernatant was collected. Titers were determined via plaque assays on Vero cells. Aliquots of viral stock were stored at -80℃. Sendai virus was propagated in 10- to 11-day-old chicken eggs that were inoculated intra-allantoically with 10^6 Sendai virus. The eggs were then incubated at 37℃ for 72 hr, and allantoic fluid was harvested and pelleted by centrifugation. The remaining allantoic fluid was aliquoted and stored at -80℃ until use.

RNA Interference Screening

RNAi screening employed an siRNA library from Dharmacon that targeted 477 annotated human genes. The screen was performed in 96-well plates. THP-1 cells were seeded in 96-well plates at a density of 50,000 and were incubated for 24 hr in 100 μl complete RPMI media containing 100 nM PMA. Differentiated THP-1 cells were treated with 60 nM siRNA complexed with 0.15 Dharmafect 4. At 72 hr, poly dA:dT with lipofectamine 2000 was added to each well. After 6 hr of incubation, the medium was harvested, and the concentration of IFN-β was measured using commercial enzyme-linked

immunosorbent assay (ELISA) kits (Antigenix America) according to the manufacturer's instructions. The experiment was performed in triplicate.

RNAi Experiment

The siRNAs were chemically synthesized by Dharmacon. The targeting sequences used were as follows: BTN3A1-1 sense, 5'-GAACAAAGCACAAGAGUGA-3'; BTN3A1-2 sense, 5'-GGAGAAGUAUCCAGUAUGC-3'; BTN3A1-3 sense, 5'-GAGAGACAUUCAGCCUAUA-3'; BTN3A1-4 sense, 5'-CUAUUUGUCCAGCGUGAAA-3'. MAP4-1 sense, 5'-GGAGUAGAAGGGAGCGAUA-3'; MAP4-2 sense, 5'-GGAGAGAUAAAGCGGGACU-3'; MAP4-3 sense, 5'-GAUGAUGUUGUGGGAGAAA-3'; and MAP4-4 sense, 5'-GAGUCAAAGAAGAAACCGU-3'. A negative control oligo was purchased from Dharmacon. HeLa cells were transfected with 40 nM siRNA using Dharmafect 1 according to the manufacturer's protocol. Differentiated THP-1 cells were treated with 60 nM siRNA via Dharmafect 4. At 72 hr transfection, the cells were used for further experiments. For shRNA treatment, double-stranded oligonucleotides corresponding to the target sequences were cloned into the pLKO.1 plasmid. Lentivirus particles were generated by co-transfecting HEK293T cells with the packaging plasmids. Supernatants were collected 48 hr later and were added to THP-1 or HeLa cells.

Cell fractionation

THP-1 cells were stimulated with poly dA:dT and harvested after 4 hr. Nuclear-cytoplasmic fractionation was conducted using a Nuclear/Cytosol fractionation kit (BioVision) according to the manufacturer's protocol.

Fluorescence Microscopy

THP-1 cells, HeLa cells or MDMs were plated onto coverslips in 12-well dishes and were grown overnight prior to stimulation with synthetic nucleic acid or inoculation with HSV-1 at the indicated times. Cells were fixed in 3.7% formaldehyde and made permeable in 0.1% Triton X-100. Coverslips were pre-incubated in 2% BSA in PBS and were stained with primary antibodies (1:100 dilution) followed with AlexaFluor 488 and AlexaFluor 568 secondary antibodies (1:400 dilution) and DAPI. Cells were analyzed with a Zeiss LSM 700 laser scanning confocal microscope.

Protein expression and purification

His-tagged mutant human BTN3A1 protein (B30.2) was expressed in *E.coli* Rosetta (λDE3) (Novagen). The Rosetta cells were grown in broth containing ampicillin at 37℃ to an OD600 of 2.0 and were rapidly cooled on ice to 16℃. After induction with 0.2 mM isopropyl-beta-d-thiogalactopyranoside (IPTG; Ducheba), the cells were allowed to grow for 24 hr at 16℃ and then were resuspended in lysis buffer and sonicated. For protein capture, recombinant

B30.2-CPD-6xHis was partially purified using an immobilized Ni^{2+} column; 250 mM imidazole was used to elute the B30.2-CPD fusion proteins. The addition of phytate activated the protease activity of CPD, and thus only recombinant B30.2 was released from the fusion proteins.

In vivo pull-down assay

HEK293T cells transfected with the indicated expression plasmids were treated with 1 μg/ml poly dA:dT or biotin-labeled poly dA:dT using PEI and were cultured for 2 hr. The cells were lysed in NP40 lysis buffer and were subjected to ultracentrifugation. Cleared lysate was incubated with streptavidin beads overnight. The beads were washed 5 times with lysis buffer, eluted with 2x sample buffer, separated on a 10% polyacrylamide gel, and analyzed by immunoblotting with anti-FLAG antibodies.

Coimmunoprecipitation and Immunoblot Analysis

HEK293T cells were transfected with the indicated plasmids using PEI for 48 hr. The cells were lysed in NP40 buffer containing protease inhibitors (100 mM PMSF, Leupeptin), and cell lysates were precipitated with a FLAG antibody overnight. On the following day, Protein G was added and incubated for 1 hr. Beads were washed 5 times with lysis buffer, and proteins were released by 2x sample buffer after boiling and then were analyzed by SDS-PAGE. For endogenous coimmunoprecipitation experiments, differentiated THP-1 cells or HeLa cells stimulated with synthetic nucleic acid using Lipofectamine 2000 were lysed in lysis buffer (15 mM Tris, 120 mM NaCl, 25 mM KCl, 2 mM EGTA, 2

mM EDTA, 0.5% Triton X-100, and 0.1 mM DTT), and the lysates were incubated with an appropriate amount of the indicated antiserum or control IgG. The subsequent procedures were carried out as described above.

Cell viability assay

Differentiated THP-1 cells were incubated with the indicated siRNA and assayed for viability 3 days later using a CellTiter Glo Luminescent Cell Viability Assay (Promega) according to the manufacturer's instructions.

Quantitative real-time PCR

THP-1 and HeLa cells were stimulated with various reagents or virus. Total RNA was extracted using Trizol reagent (Life Technologies) and reverse transcribed with ReverTraAce (Toyobo) according to the manufacturer's instructions. Real-time PCR was performed using the following primers: hIFNβ, sense 5'-ATGACCAACAAGTGTCTCCTCC-3', reverse 5'-GCTCATGGAAAGAGCTGTAGTG-3'; hβ-actin, sense 5'-CATGTACGTTGCTATCCAGGC-3', reverse 5'-CTCCTTAATGTCACGCACGAT-3'; hTNF-α, sense 5'-TCCTACCAGACCAAGGTCAA-3', reverse 5'-AGACCCCTCCCAGATAGATG-3'; hBTN3A1, sense 5'-TTTCCATCGCAGACCCCTTC-3', reverse 5'-TCCTCCAGGAGCTTCACTCT-3'; hBTN1A1, sense 5'-TAGTGGCTGTGGCTGTCATC-3', reverse 5'-TCAACTGCATGCAAGGTAGC-3'; hBTN2A1, sense 5'-CCACGGTTGGAGAAAACACT-3', reverse 5'-GTTTTCCTGGGCTGTGATGT-

3’ ; hBTN2A2, sense 5’ - TCCTCCTTCTCAGCCTGTGT-3’ , reverse 5’ - TCCTCCATCTGCTCCTCTGT-3 ’ ; hBTN3A3, sense 5 ’ - CTCTCACTGAGCCCAGAACC-3’ , reverse 5’ - AGGATCGGGGGAACTCTCTA-3’ ; hOasL, sense 5’ - GGACCGTGGAGGAGTTTCTG-3’ , reverse 5’ - GAGCCCACCTTGACTACCTTC-3 ’ ; hIP-10, sense 5 ’ - TGACTCTAAGTGGCATTCAAGGAG-3 ’ , reverse 5 ’ - TTTTTCTAAAGACCTTGGATTAACAGG-3 ’ ; hIFITM1, sense 5 ’ - CCCCCAGCACCATCCTTC-3 ’ , reverse 5 ’ - ACCCCGTTTTTCCTGTATTATCTGT-3 ’ ; hMxA, sense 5 ’ - AGGTCAGTTACCAGGACTAC-3’ , reverse 5’ - ATGGCATTCTGGGCTTTATT-3’ ; and hMAP4, sense 5’ - CAC TCC TAG CCA ATG GTG GT-3’ , reverse 5’ - GTA TCA GCT GTC GCA CTG GA-3’ .

Time-dependent imaging in live cells

The fluorescent signals in HeLa cells transfected with GFP or BTN3A1-GFP were observed after treatment with synthetic DNA using an IN Cell Analyzer 2000 (GE Healthcare Life Sciences, USA) with 20X objective lenses (Olympus, Japan) at various time points (0 – 120 min). Green fluorescence ($\lambda_{ex}/\lambda_{em}$=495/521) in the cells was monitored every 20 minutes, and blue fluorescence ($\lambda_{ex}/\lambda_{em}$=358/461) from the nuclei was observed after Hoechst33342 treatment at two hours. The cells were incubated and preserved at 37° C in 5% CO_2 for real-time imaging. The acquisition images were modified by pseudo-coloring, fluorescence intensity and background elimination processes using the software supplied with the IN Cell Analyzer 2000.

Generation of BTN3A1 knockout cell lines

We used the CRISPR/Cas9 genome editing system to generate BTN3A1 knockout HeLa cells. We used a lentiviral CRISPR/Cas9 vector. Five pairs of sgRNA targeting BTN3A1 were designed and transfected into HEK293T cells. Two days after transfection, we collected the supernatants with lentiviral particles. The lentiviral supernatants were transferred into HeLa cells. HeLa cells were selected with 1μg/ml puromycin for 1 week. Cells were subsequently cloned by limiting dilution, and individual clones were subjected to immunoblotting to confirm the depletion of the target protein, BTN3A1. The genomic DNA was also extracted from each clone for PCR amplification. Targeted cleavage was evaluated at the endogenous loci by T7E1 assay. To further determine the mutational spectra, amplification bands were cloned using the TOPcloner Blunt core kit (Enzynomics), and then Sanger sequenced to verify the individual mutations.

Statistical analyses

GraphPad Prism version 5.0 software was used (GraphPad Software, San Diego, CA). All values are expressed as the mean ±s.d. Differences were determined to be significant at $P<0.05$, by the two-tailed Student's t-test.

VI. REFERENCES

1. Garcia-Sastre, A. and C.A. Biron, *Type 1 interferons and the virus-host relationship: a lesson in detente.* Science, 2006. **312**(5775): p. 879-82.
2. Theofilopoulos, A.N., et al., *Type I interferons (alpha/beta) in immunity and autoimmunity.* Annu Rev Immunol, 2005. **23**: p. 307-36.
3. Medzhitov, R., P. Preston-Hurlburt, and C.A. Janeway, Jr., *A human homologue of the Drosophila Toll protein signals activation of adaptive immunity.* Nature, 1997. **388**(6640): p. 394-7.
4. Akira, S., S. Uematsu, and O. Takeuchi, *Pathogen recognition and innate immunity.* Cell, 2006. **124**(4): p. 783-801.
5. Kato, H., K. Takahasi, and T. Fujita, *RIG-I-like receptors: cytoplasmic sensors for non-self RNA.* Immunol Rev, 2011. **243**(1): p. 91-8.
6. Keating, S.E., M. Baran, and A.G. Bowie, *Cytosolic DNA sensors regulating type I interferon induction.* Trends Immunol, 2011. **32**(12): p. 574-81.
7. Martinon, F. and J. Tschopp, *NLRs join TLRs as innate sensors of pathogens.* Trends Immunol, 2005. **26**(8): p. 447-54.
8. Yoneyama, M. and T. Fujita, *RNA recognition and signal transduction by RIG-I-like receptors.* Immunol Rev, 2009. **227**(1): p. 54-65.
9. Hornung, V., et al., *5'-Triphosphate RNA is the ligand for RIG-I.* Science, 2006. **314**(5801): p. 994-7.
10. Kato, H., et al., *Differential roles of MDA5 and RIG-I helicases in the recognition of RNA viruses.* Nature, 2006. **441**(7089): p. 101-5.
11. Kondo, T., et al., *DNA damage sensor MRE11 recognizes cytosolic*

double-stranded DNA and induces type I interferon by regulating STING trafficking. Proc Natl Acad Sci U S A, 2013. **110**(8): p. 2969-74.

12. Sun, L., et al., *Cyclic GMP-AMP synthase is a cytosolic DNA sensor that activates the type I interferon pathway.* Science, 2013. **339**(6121): p. 786-91.
13. Unterholzner, L., et al., *IFI16 is an innate immune sensor for intracellular DNA.* Nat Immunol, 2010. **11**(11): p. 997-1004.
14. Zhang, Z., et al., *The helicase DDX41 senses intracellular DNA mediated by the adaptor STING in dendritic cells.* Nat Immunol, 2011. **12**(10): p. 959-65.
15. Ishikawa, H. and G.N. Barber, *STING is an endoplasmic reticulum adaptor that facilitates innate immune signalling.* Nature, 2008. **455**(7213): p. 674-8.
16. Ishikawa, H., Z. Ma, and G.N. Barber, *STING regulates intracellular DNA-mediated, type I interferon-dependent innate immunity.* Nature, 2009. **461**(7265): p. 788-92.
17. Seth, R.B., et al., *Identification and characterization of MAVS, a mitochondrial antiviral signaling protein that activates NF-kappaB and IRF 3.* Cell, 2005. **122**(5): p. 669-82.
18. Fitzgerald, K.A., et al., *IKKepsilon and TBK1 are essential components of the IRF3 signaling pathway.* Nat Immunol, 2003. **4**(5): p. 491-6.
19. Arnett, H.A. and J.L. Viney, *Immune modulation by butyrophilins.* Nat Rev Immunol, 2014. **14**(8): p. 559-69.
20. Abeler-Dorner, L., et al., *Butyrophilins: an emerging family of immune regulators.* Trends Immunol, 2012. **33**(1): p. 34-41.
21. Smith, I.A., et al., *BTN1A1, the mammary gland butyrophilin, and*

BTN2A2 are both inhibitors of T cell activation. J Immunol, 2010. **184**(7): p. 3514-25.

22. Robenek, H., et al., *Butyrophilin controls milk fat globule secretion.* Proc Natl Acad Sci U S A, 2006. **103**(27): p. 10385-90.
23. Malcherek, G., et al., *The B7 homolog butyrophilin BTN2A1 is a novel ligand for DC-SIGN.* J Immunol, 2007. **179**(6): p. 3804-11.
24. Arnett, H.A., S.S. Escobar, and J.L. Viney, *Regulation of costimulation in the era of butyrophilins.* Cytokine, 2009. **46**(3): p. 370-5.
25. Ammann, J.U., A. Cooke, and J. Trowsdale, *Butyrophilin Btn2a2 inhibits TCR activation and phosphatidylinositol 3-kinase/Akt pathway signaling and induces Foxp3 expression in T lymphocytes.* J Immunol, 2013. **190**(10): p. 5030-6.
26. Compte, E., et al., *Frontline: Characterization of BT3 molecules belonging to the B7 family expressed on immune cells.* Eur J Immunol, 2004. **34**(8): p. 2089-99.
27. Harly, C., et al., *Key implication of CD277/butyrophilin-3 (BTN3A) in cellular stress sensing by a major human gammadelta T-cell subset.* Blood, 2012. **120**(11): p. 2269-79.
28. Yamashiro, H., et al., *Stimulation of human butyrophilin 3 molecules results in negative regulation of cellular immunity.* J Leukoc Biol, 2010. **88**(4): p. 757-67.
29. Le Page, C., et al., *BTN3A2 expression in epithelial ovarian cancer is associated with higher tumor infiltrating T cells and a better prognosis.* PLoS One, 2012. **7**(6): p. e38541.
30. Bas, A., et al., *Butyrophilin-like 1 encodes an enterocyte protein that selectively regulates functional interactions with T lymphocytes.* Proc

Natl Acad Sci U S A, 2011. **108**(11): p. 4376-81.

31. Yamazaki, T., et al., *A butyrophilin family member critically inhibits T cell activation.* J Immunol, 2010. **185**(10): p. 5907-14.
32. Arnett, H.A., et al., *BTNL2, a butyrophilin/B7-like molecule, is a negative costimulatory molecule modulated in intestinal inflammation.* J Immunol, 2007. **178**(3): p. 1523-33.
33. Nguyen, T., et al., *BTNL2, a butyrophilin-like molecule that functions to inhibit T cell activation.* J Immunol, 2006. **176**(12): p. 7354-60.
34. Chapoval, A.I., et al., *BTNL8, a butyrophilin-like molecule that costimulates the primary immune response.* Mol Immunol, 2013. **56**(4): p. 819-28.
35. Barbee, S.D., et al., *Skint-1 is a highly specific, unique selecting component for epidermal T cells.* Proc Natl Acad Sci U S A, 2011. **108**(8): p. 3330-5.
36. Yang, Y., et al., *Characterization of B7S3 as a novel negative regulator of T cells.* J Immunol, 2007. **178**(6): p. 3661-7.
37. Caviston, J.P. and E.L. Holzbaur, *Microtubule motors at the intersection of trafficking and transport.* Trends Cell Biol, 2006. **16**(10): p. 530-7.
38. Chiang, H.S., et al., *GEF-H1 controls microtubule-dependent sensing of nucleic acids for antiviral host defenses.* Nat Immunol, 2014. **15**(1): p. 63-71.
39. Mori, M., et al., *Identification of Ser-386 of interferon regulatory factor 3 as critical target for inducible phosphorylation that determines activation.* J Biol Chem, 2004. **279**(11): p. 9698-702.
40. Liu, S., et al., *Phosphorylation of innate immune adaptor proteins MAVS, STING, and TRIF induces IRF3 activation.* Science, 2015. **347**(6227): p.

aaa2630.

41. Vavassori, S., et al., *Butyrophilin 3A1 binds phosphorylated antigens and stimulates human gammadelta T cells.* Nat Immunol, 2013. **14**(9): p. 908-16.

42. Wang, H., et al., *Butyrophilin 3A1 plays an essential role in prenyl pyrophosphate stimulation of human Vgamma2Vdelta2 T cells.* J Immunol, 2013. **191**(3): p. 1029-42.

43. Semenova, I., et al., *Regulation of microtubule-based transport by MAP4.* Mol Biol Cell, 2014. **25**(20): p. 3119-32.

44. Hagiwara, H., et al., *Competition between motor molecules (kinesin and cytoplasmic dynein) and fibrous microtubule-associated proteins in binding to microtubules.* J Biol Chem, 1994. **269**(5): p. 3581-9.

45. Lopez, L.A. and M.P. Sheetz, *Steric inhibition of cytoplasmic dynein and kinesin motility by MAP2.* Cell Motil Cytoskeleton, 1993. **24**(1): p. 1-16.

46. Drewes, G., A. Ebneth, and E.M. Mandelkow, *MAPs, MARKs and microtubule dynamics.* Trends Biochem Sci, 1998. **23**(8): p. 307-11.

47. Mandell, J.W. and G.A. Banker, *Microtubule-associated proteins, phosphorylation gradients, and the establishment of neuronal polarity.* Perspect Dev Neurobiol, 1996. **4**(2-3): p. 125-35.

48. Diao, F., et al., *Negative regulation of MDA5- but not RIG-I-mediated innate antiviral signaling by the dihydroxyacetone kinase.* Proc Natl Acad Sci U S A, 2007. **104**(28): p. 11706-11.

49. Zhong, B., et al., *The ubiquitin ligase RNF5 regulates antiviral responses by mediating degradation of the adaptor protein MITA.* Immunity, 2009. **30**(3): p. 397-407.

50. Tsuchida, T., et al., *The ubiquitin ligase TRIM56 regulates innate*

immune responses to intracellular double-stranded DNA. Immunity, 2010. **33**(5): p. 765-76.

51. Hayakawa, S., et al., *ZAPS is a potent stimulator of signaling mediated by the RNA helicase RIG-I during antiviral responses.* Nat Immunol, 2011. **12**(1): p. 37-44.

52. Kawasaki, T., T. Kawai, and S. Akira, *Recognition of nucleic acids by pattern-recognition receptors and its relevance in autoimmunity.* Immunol Rev, 2011. **243**(1): p. 61-73.

53. Misawa, T., et al., *Microtubule-driven spatial arrangement of mitochondria promotes activation of the NLRP3 inflammasome.* Nat Immunol, 2013. **14**(5): p. 454-60.

54. Avila, J., J. Dominguez, and J. Diaz-Nido, *Regulation of microtubule dynamics by microtubule-associated protein expression and phosphorylation during neuronal development.* Int J Dev Biol, 1994. **38**(1): p. 13-25.

55. Dobbs, N., et al., *STING Activation by Translocation from the ER Is Associated with Infection and Autoinflammatory Disease.* Cell Host Microbe, 2015. **18**(2): p. 157-68.

VII. ABSTRACT IN KOREAN

선천적 면역 체계는 바이러스의 핵산을 인지하고 인터페론 반응을 일으킨다. RNA와 DNA를 인지하는 수용체는 다르지만 최종적으로는 인산전달효소인 TBK1과 전사 인자인 IRF3로 모인다. 인터페론 반응은 핵심 신호 전달 단백질을 핵 근처로 이동시키게 되는데, 이러한 공간적인 이동 조절이 어떠한 매개자에 의해서 이루어지는지 아직까지 밝혀지지 않았다. 본 연구는 핵산에 의해 유도되는 인터페론 반응에서 양성적 조절자로써 BTN3A1을 동정해냈다. BTN3A1의 결손은 세포질에 존재하고 있는 핵산에 의해 유도되는 인터페론의 생산을 저해한다. 비활성 상태에서 BTN3A1은 계속적으로 TBK1과 결합하고 있다. 하지만, 핵산에 의해 활성화되면 BTN3A1-TBK1의 복합체가 핵 근처로 이동하고 그 곳에서 BTN3A1은 TBK1과 IRF3의 결합을 매개하고 이에 따라 IRF3의 인산화를 유도한다. 또한 핵산 자극 반응의 하나로 다이네인에 의한 BTN3A1의 이동을 MAP4가 조절하고 있다는 것을 밝혔다. 따라서 DNA나 RNA와 같은 핵산에 의한 인터페론 반응에서 MAP4와 BTN3A1이 중요한 역할을 하고 있다는 것을 알아내었다. 이 연구를 통해 MAP4와 BTN3A1이 핵산 매개 면역 반응에서 중심적인 기능을 하는 TBK1을 이동시키는데 있어 결정적인 역할을 하고 있다는 것을 증명하였다.

주요어: BTN3A1, MAP4, 다이네인, 인터페론 반응

학번: 2010-30934